The effect of glyphosate on bacteria and archaea community composition in freshwater biofilms

by

Lauren Elizabeth Koiter

A thesis

presented to the University of Waterloo

in fulfillment of the

thesis requirement for the degree of

Master of Science

in

Biology (Water)

Waterloo, Ontario, Canada, 2022

AUTHOR'S DECLARATION

I hereby declare that I am the sole author of this thesis. This is a true copy of the thesis, including any required final revisions, as accepted by my examiners.

I understand that my thesis may be made electronically available to the public.

Statement of Contributions

This thesis, consisting of one manuscript, is written by Lauren Koiter and supervised by Dr. Rebecca Rooney. Dr. Kirsten Müller and Dr. Trevor Charles attended as committee members for this thesis.

I, Lauren Koiter, am the sole author of this thesis and am responsible for the study design, field work planning and implementation, lab experiment planning and implementation, drafts of all chapters of this thesis, and final submission of this thesis to the University of Waterloo, Department of Biology in fulfillment of the requirements of the degree Master of Science.

I received field and lab assistance from Dr. Laura Beecraft, Hillary Quinn-Austin, Calvin Lei, Catriona Leven, Owen Royall, Jordan Reynolds, Jessie Pearson, Sarah Yuckin, Jacob Basso, Julia Weder, Matthieu Tanguay and Joanna Majarreis.

Extraction and sequencing of genetic samples was completed by Dr. Jiujun Cheng, University of Waterloo, Department of Biology.

Bioinformatics and preliminary analysis of genetic samples was completed by Dr. Michael Lynch, MetagenomBio Inc.

I received advice and support for my analysis from Dr. Kirsten Müller, Dr. Trevor Charles, Dr. Andrew Doxey, Dr. Ellen Cameron, and Adrian Van Dyke.

I also received advice in statistical analyses methods from Dr. Rebecca Rooney and Dr. Laura Beecraft.

Additional feedback on drafts was provided by Dr. Laura Beecraft and Dr. Rebecca Rooney. Dr. Michael Lynch provided feedback on the description of sequencing methods and results.

Throughout this thesis I will be using the collective term "we" to acknowledge the various contributions that made this thesis possible.

Abstract

Glyphosate-based herbicides are some of the most widely used herbicides in the world today, however, there is still much to learn about how glyphosate affects non-target ecosystems. Specifically, freshwater aquatic biofilms are often exposed to glyphosate-based herbicides through anthropogenic activities. This study aims to understand the effects of glyphosate on bacteria and archaea components of freshwater biofilms through a simulated agricultural pulse-dose exposure of 0.5 mg glyphosate a.e./L biweekly over 21 days. Biofilms were cultured *in situ* from a variety of wetlands in Rondeau Bay, Ontario and were transported to lab microcosms for the exposure experiment. We found that glyphosate exposure did not have a significant effect on the richness or Shannon-Weiner diversity of bacteria or archaea within biofilm communities. These communities did significantly change over time due to glyphosate exposure, but the exposure did not drive the microbial communities toward greater homogeneity or heterogeneity in composition. We also found evidence that amplicon sequence variants that were indicative of glyphosate-exposed communities may be resistant to glyphosate through class II EPSPS enzymes and some may be able to use glyphosate as a phosphorus source through C-P lyase. This suggests that biofilm communities are structurally resilient to pulsed exposures of glyphosate over chronic exposure durations at realistic environmental exposure levels. Additionally, some bacteria or archaea may be useful indicators of episodic glyphosate contamination in wetland ecosystems. Given their complexity, ubiquity, and functional importance in shallow waters, biofilm ecology is a growing field of study.

Acknowledgements

Table of Contents

List of Figures

List of Tables

<div align="center">

Chapter 1

Introduction

</div>

1.1 Biofilm: Definition and Importance in Aquatic Ecosystems

Aquatic biofilms are comprised of algae, bacteria, archaea, fungi, and other microorganisms that form surface-attached aggregates (Wu, 2017). Biofilms often form the base of aquatic food chains in shallow water systems and can be found almost universally in aquatic ecosystems (Vera et al., 2009). In addition, biofilms also play a key role in nutrient cycling; especially for carbon, nitrogen, and phosphorus cycles (Pérez et al., 2011; Wu, 2017). The effect of anthropogenic contaminants on bacteria and archaea in biofilms is an important field of study because of the effects these microorganisms can have on ecosystem functions, including contaminant removal. Freshwater biofilms have been shown to bioconcentrate anthropogenic contaminants such as glyphosate (Beecraft & Rooney, 2020) and bacteria in biofilms are known to play a role in the biodegradation of glyphosate (Carles et al., 2019; Hove-Jensen et al., 2014; Sviridov et al., 2015). However, the potential effect of environmental exposure to glyphosate on biofilm bacteria and archaea community composition is not well studied. This knowledge gap is important, as changes to the bacterial and archaeal components of the biofilm community could have ramifications for the structure and function of the biofilm itself, as well as broader ecological implications.

The colonization of biofilms on an aquatic surface begins with bacteria (Wahl, 1989; Wu, 2017). For example, Wahl (1989) notes that rod-shaped bacteria typically colonize first, followed by coccoid and filamentous shapes. A key component of biofilm structure is enclosing polysaccharides called the extracellular polymeric substance (Khadra et al., 2018). Bacteria begin the secretion of the extracellular polymeric substance that allows other organisms to attach to the community surface (Wahl, 1989; Wu, 2017). This layer is required for structural stability in the community as it holds organisms together and protects mature communities from some stressors (Khadra et al., 2018). Bacteria and archaea within biofilm communities are very diverse, with an estimated 40-80% of all cells on Earth residing within biofilm communities (Flemming & Wuertz, 2019). Unfortunately, Flemming & Wuertz (2019) do not separate these two domains, but clearly biofilms are a crucial habitat for microbes.

Algae and cyanobacteria are among the last to colonize a biofilm community, but often play the most significant role in overall structure and appearance of the community (Wahl, 1989; Wu,

<div align="center">

1

</div>

31 2017). Biofilms can be very diverse in appearance due to variations in algal composition, ranging

32 from brown to green, dense to sparse, and slimy to rough (Wu, 2017). These variations are driven by

33 environmental factors such as temperature, light, nutrient availability, depth, and water flow (Wu,

34 2017, and references therein). In addition to influencing the appearance of the biofilm, algae and

35 cyanobacteria carry out photosynthesis, altering community metabolism and nutrient cycling

36 functions (Romaní et al., 2004).

37   Biofilm communities are especially important in shallow rivers and lakes because these

38 systems have more surface area on submersed macrophyte tissues and other substrates that are

39 exposed to sufficient light to support biofilm development; however, these ecosystems are also at a

40 greater risk of disturbance, where stressors such as chemical, temperature, or flow change would have

41 a much greater impact on the communities (Vera et al., 2009; Wu, 2017). For example, nutrient

42 pollution can lead to increases in autotrophic production that decrease the diversity within a biofilm

43 as certain taxa outcompete others that cannot take advantage of the nutrient loading (Roberto et al.,

44 2018; Wu, 2017). As such, these communities can be used as bioindicators of water quality in areas

45 that have runoff from areas of high nutrient input (Lavoie et al., 2004; Montuelle et al., 2010;

46 Moresco & Rodrigues, 2014). Furthermore, changes in the biofilm community can influence the

47 broader function of freshwater ecosystems. Loss or alteration of these biofilm communities due to

48 stressors could change the surrounding aquatic ecosystem due to the key role biofilms play in aquatic

49 nutrient cycling and food chains (Pérez et al., 2011; Wu, 2017). For example, high nutrient inputs due

50 to anthropogenic activities can contribute to rapid growth of algae and cyanobacteria within biofilm

51 communities (Lu et al., 2016). This promotes nuisance algae growth and disrupts freshwater food

52 webs as fatty acid and stable isotope tracer studies reveal the dietary dependence of freshwater

53 metazoans on the algae in biofilms (Vadeboncoeur & Power, 2017, and references therein). Thus,

54 changes to biofilms can impact whole ecosystems.

1.1 Glyphosate: Definition and Occurrence in Aquatic Ecosystems and Relation to Biofilms

55

56

57   Glyphosate, also called *N*[phosphonomethyl] glycine, is one of the most commonly used

58 herbicides in the world (e.g., formulations of Roundup®), accounting for 54% of all pesticide use in

59 Ontario between 2013 and 2014 (Farm & Food Care Ontario, 2015). This herbicide is commonly used

60   in agriculture due to the production and widespread distribution of genetically modified plants that

61   are resistant to glyphosate (Battaglin et al., 2014; Khadra et al., 2018; Primost et al., 2017).

62   Glyphosate is a broad-spectrum herbicide that targets aromatic amino acid production by

63   inhibiting the 5-enolpyruvylshikimic acid-3-phosphate synthase (EPSPS) in most plants and some

64   bacteria (Battaglin et al., 2014; Khadra et al., 2018; Pérez et al., 2011; Pollegioni et al., 2011;

65   Steinrucken & Amrhein, 1980; Tohge et al., 2013). The primary targeted aromatic amino acids are

66   phenylalanine, tyrosine, and tryptophan which are required in the production of proteins (Battaglin et

67   al., 2014; Khadra et al., 2018).

68   The EPSPS pathways are divided into two main classes: class I is sensitive to glyphosate with

69   amino acid synthesis being inhibited, and class II is not sensitive to glyphosate with amino acid

70   synthesis being unaffected (Pollegioni et al., 2011; Tohge et al., 2013; Van Bruggen et al., 2018).

71   Some crop plants have been genetically modified to be resistant to glyphosate for agricultural

72   purposes (Pollegioni et al., 2011), but this has led to some agricultural weeds evolving to possess

73   glyphosate resistance after prolonged exposure to this herbicide (Waltz, 2010). Indeed, the class II

74   EPSPS pathway used in genetically modified commercial crops is synthesized from a variety of

75   naturally occurring mutations in some bacteria that confer glyphosate resistance (Pollegioni et al.,

76   2011).

77   Glyphosate resistant organisms can therefore benefit from glyphosate contamination in the

78   environment. For example, some species of cyanobacteria with the class II EPSPS pathway are

79   known to use glyphosate as a phosphorus source when it is broken down microbially to release

80   orthophosphate (Khadra et al., 2018; Van Bruggen et al., 2018). These organisms are also able to use

81   nutrients released by glyphosate-sensitive organisms as they die off (Van Bruggen et al., 2018). The

82   breakdown products of both glyphosate and glyphosate-sensitive organisms may allow glyphosate

83   resistant organisms to thrive in contaminated ecosystems.

84   Glyphosate application is typically restricted to use over land, with buffers to protect aquatic

85   ecosystems from exposure (PMRA, 2017); yet, runoff, wind fallout, and overspray can cause the

86   chemical to enter aquatic ecosystems (Benbrook, 2016; Khadra et al., 2018; Maggi et al., 2020).

87   'Water-safe' formulations of glyphosate (e.g., Glyphosate 5.4 by Alligare in the USA or Roundup®

88   Custom by Bayer Crop Science in the USA) are used directly over water to control invasive

89   *Phragmites australis* on the shores of the Laurentian Great Lakes (Breckels & Kilgour, 2018;

3

90 Robichaud & Rooney, 2021). Glyphosate applied in this manner has been documented to

91 bioconcentrate in biofilms (Beecraft & Rooney, 2020); however, the effects on biofilm community

92 structure have not yet been assessed.

93   Pure glyphosate is largely thought to have low toxicity in humans and other mammals due to

94 a lack of EPSPS pathways (Tohge et al., 2013). However, glyphosate is sold in many different

95 products, combined with different adjuvants (surfactants, anti-foaming agents, dyes, etc.) to create

96 formulations that differ strongly in their toxicity to aquatic organisms (Mesnage et al., 2019; Tsui &

97 Chu, 2003). Many of these formulations are proprietary, leading to confusion and uncertainty as to

98 whether effects of herbicides observed can be attributed to glyphosate itself or to unknown additives

99 (Mesnage et al., 2018). Some studies have compared glyphosate formulations, finding increased

100 toxicity in commercial formulations due to additives (Mesnage et al., 2019; Pérez et al., 2011; Tsui &

101 Chu, 2003). Studies have noted that glyphosate use in agriculture can affect many non-target

102 organisms, including fish, spiders, and root zone microbes; though the effect may be compounded by

103 the surfactants and adjuvants (Battaglin et al., 2014, and references therein). Ecotoxicological studies

104 have tested the responses of animals and invertebrates to glyphosate (Annett et al., 2014; Breckels &

105 Kilgour, 2018), but the effect on bacteria and archaea within biofilms is uncertain.

106   It is difficult to compare between studies due to variation in the forms and formulations of

107 glyphosate used (Mesnage et al., 2019); for example, comparing between pure glyphosate acid or

108 salts (Szekacs & Darvas, 2012; Vera et al., 2014). These factors have often led to conflicting results.

109 Variability in results can also occur with variations in the concentration of glyphosate, duration of

110 exposure, and response variables measured (Annett et al., 2014; Battaglin et al., 2014). It is important

111 to consider the formulation of glyphosate when comparing ecotoxicological research results

112 (Mesnage et al., 2019).

113   Research into the effects of glyphosate on algae in biofilms has a long history (e.g.,

114 Goldsborough & Brown, 1988) and is ongoing (Vera et al., 2014; Beecraft et al., IN REVIEW), but

115 its effects on bacteria and archaea within biofilms is not as well studied (but see Carles & Artigas,

116 2020). Some studies have looked specifically into biofilm exposure to glyphosate; however, these

117 studies were almost all conducted with the addition of a second variable such as the effect of biofilm

118 maturity on glyphosate exposure response of biofilms (Khadra et al., 2018), invasive species in

119   conjunction with glyphosate (Pizarro et al., 2016), or a secondary herbicide compared to glyphosate

120   (Barbosa da Costa et al., 2021; Gattás et al., 2016; Lozano et al., 2018).

121   Of the studies that have investigated the bacteria and archaea response to glyphosate

122   exposure, prominent are two that have simulated the conditions of the agricultural Pampa plain in

123   Argentina using outdoor lake mesocosms (Pérez et al., 2011; Vera et al., 2009). These studies found

124   that cyanobacteria abundance significantly increased following glyphosate exposure (Lozano et al.,

125   2018; Pérez et al., 2007; Vera et al., 2009). This is likely because some cyanobacteria species are

126   known to have the class II EPSPS which would allow these species to survive glyphosate exposure

127   (Khadra et al., 2018). Some of these cyanobacteria with the class II EPSPS are also known to use the

128   breakdown products of glyphosate as a phosphorus source, allowing them to outcompete other

129   species in glyphosate contaminated ecosystems (Khadra et al., 2018). Other species of bacteria were

130   found to have no significant changes to abundance following glyphosate exposure, especially in

131   heterotrophic bacterioplankton species (Pérez et al., 2007). However, the Pampa plain studies used

132   high concentrations of glyphosate (e.g. 7.8-39 mg a.e./L Kish, 2006; 6-12 mg a.e./L Pérez et al.,

133   2007; 8 mg a.e./L Vera et al., 2009; 1-6 mg a.e./L Pizarro et al., 2016) . While these concentrations

134   may be more common of environmental monitoring in Argentina, they are unrealistic exposure

135   concentrations in North America. Glyphosate is frequently detected in surface waters of North

136   America, but observed concentrations ranging typically from <0.02 µg a.e. /L to 1.95 mg a.e. /L

137   (Annett et al., 2014; Benbrook, 2016; Medalie et al., 2020). It is important to use environmentally

138   relevant concentrations in ecotoxicological studies to understand the effects that natural communities

139   are likely to experience in the environment.

140   Some studies on the effects of glyphosate on biofilm bacteria and archaea have been

141   conducted using environmentally relevant concentrations, yet most have short time series, ranging

142   from a few hours to around seven days (e.g., Khadra et al., 2018; Lozano et al., 2018). These short-

143   term exposure studies are effective for studying the acute responses of organisms to glyphosate

144   exposure, but their environmental relevance is compromised because biofilms in the natural

145   environment are exposed to repeated (pulsed) doses of glyphosate over many years (Chow et al.,

146   2020). Not only are realistic exposure concentrations important, but also realistic durations of

147   exposure to understand what effects environmental contamination of freshwater ecosystems with

148   glyphosate is likely to have on aquatic biota. There have been chronic-duration studies conducted on

149   the effect of glyphosate on bacterioplankton (Barbosa da Costa et al., 2021), but it is unclear to what

150 extent glyphosate would affect bacteria within biofilms, which benefit from the protection afforded
151 by the extracellular polymeric substance (Wu, 2017).

152   Different organisms have known variation in their tolerance to glyphosate exposure. For
153 example, Perez et al. 2011, and references therein, report variability in concentration tolerance
154 observed in aquatic species of bacteria and other protozoa. The green alga *Chlorella* showed a 50%
155 reduction in function (EC50) after 600 mg a.e./L exposure while the diatom *Skeletonema* had a 50%
156 reduction in function (EC50) after only 0.68 mg a.e./L (Christy et al., 1981; Pérez et al., 2011). Due
157 to this variability among species in terms of their tolerance for glyphosate, we predict certain changes
158 in community composition will follow from long-term exposure at environmentally relevant
159 concentrations. These changes may be studied using molecular sequencing techniques. For example,
160 in biofilms chronically exposed to glyphosate we would expect to see an increase in cyanobacteria
161 that may possess the class II EPSPS that could outcompete algal species that may be sensitive to
162 glyphosate.

163   In addition to direct responses to glyphosate exposure predicted to occur in sensitive
164 organisms, some taxa may exhibit a delayed response to the glyphosate-caused community changes.
165 For example, macrophytes have a lower tolerance to glyphosate than other aquatic organisms (Pérez
166 et al., 2011). Therefore, while low exposure to glyphosate may have a reduced effect on
167 microorganisms within biofilms, the cascading effect of alteration in other areas of the ecosystem
168 may have a delayed impact on biofilm communities through the influx of additional nutrients as
169 affected organisms decompose.

170

171 1.2 Bacteria in Aquatic Biofilms Molecular Relationship to Glyphosate

172   Pure glyphosate is a phosphonic acid that is broken down or catabolized by microorganisms
173 in one of two ways: through cleavage at the carbon-phosphorus bond through C-P lyase resulting in
174 sarcosine and a phosphorus molecule, or through cleavage at the carboxymethylene-nitrogen bond
175 resulting in aminomethylphosphonic acid (AMPA) and glyoxylate (Hove-Jensen et al., 2014;
176 Sviridov et al., 2015). The complete biodegradation of glyphosate to release bioavailable phosphorus
177 requires several reactions mediated by the C-P lyase enzymatic pathway (Hove-Jensen et al., 2014).
178 Microorganisms with the class II EPSPS that also contain a C-P lyase may be able to degrade

179   glyphosate and use it as a phosphorus source (Sviridov et al., 2015), allowing for the dominance of

180   species with these proteins in environments with chronic glyphosate exposure.

181   The EPSPS class in bacteria has been linked to mutations in codon 106 of the genetic

182   sequence which contain known protein variations related to the enzyme class (Leino et al., 2021;

183   Nandula et al., 2018). The class I glyphosate-sensitive organisms have a proline at codon 106, while

184   variation away from proline would indicate a class II glyphosate-resistant organism (Nandula et al.,

185   2018). Short of directly sequencing the EPSPS gene from biofilm samples, we can investigate

186   evidence of variations in codon 106 with 16S amplicon sequencing, if the amplicon sequence variants

187   can be identified to the species-level and matched with fully sequenced genomes in nucleotide

188   sequence databases (e.g. GenBank or RefSeq), i.e., using a Basic Local Alignment Search Tool

189   (BLAST) (Altschul et al., 1990). One hinderance to this indirect approach is that natural communities

190   often have numerous species that are not fully sequenced or taxonomically defined, limiting the

191   number of organisms that can be tested for the EPSPS class proteins.

192   Variations of the C-P lyase pathway can be found in many microorganisms. It comprises a

193   series of protein sequences regulated by multiple genes organized into the *phn* operon (Stosiek et al.,

194   2020). The *phn* operon contains multiple genes, with variation in the presence, order, and abundance

195   of these genes among species (Hove-Jensen et al., 2014; Stosiek et al., 2020). A complex of genes,

196   *phnGHIJKLM* is considered required for functional C-P lyase (Stosiek et al., 2020), with *phnJ* coding

197   for the C-P lyase enzyme, while the *phnGHK* provide supporting enzymes and proteins for the

198   functional C-P lyase pathway (Hove-Jensen et al., 2014). Careful consideration must be taken when

199   assessing for C-P lyase functionality because some organism may have *phn* genes present in their

200   genome without the full operon able to confer functional C-P lyase (Hove-Jensen et al., 2014).

201   Similar to the approach described above for indirectly evaluating the presence of variations in codon

202   106 suggestive of glyphosate resistance among ASVs that can be matched with genomes in

203   nucleotide sequence databases, we can seek evidence of the genes necessary for C-P lyase among

204   ASVs matched to taxa defined and sequenced in such databases.

205

1.3 Objectives

Our objectives are to assess the effects of glyphosate exposure on the bacteria and archaea component of freshwater biofilm communities. To maximize realism, we delivered an environmentally realistic concentration of glyphosate in a repeated pulse over a period of three weeks, analogous to the way storm events might supply glyphosate laden run-off to a wetland (Chow et al., 2020). We also used Roundup® Custom by Bayer Crop Science (obtained from the USA), because this product is applied directly to standing water and contains no adjuvants that could confound the attribution of any observed effects to glyphosate per se. It contains glyphosate in the form of an isopropyl amine salt (CAS 38641-94-0), which is the most common form used in agricultural applications of glyphosate-based herbicide.   Specifically, we sought to test for (i) changes in bacteria and archaea community composition following twenty-one days of bi-weekly additions of glyphosate, and (ii) the presence of genetic sequences indicating potential biological resistance to glyphosate and/or the ability to use glyphosate as a phosphorus source. We hypothesize that (i) repeated pulses of glyphosate over a 21-day period will result in changes to the community composition of bacteria and archaea in wetland biofilms. For example, we predict that cyanobacteria should become more common as previous research has found these organisms to be more tolerant of glyphosate contamination than other taxa (e.g. Forlani et al., 2008; Powell et al., 1991). We hypothesize that (ii) amplicon sequence variants (ASVs) that increase in proportionate abundance in glyphosate exposed biofilms will be more likely to exhibit mutations in the codon 106 of the EPSPS gene, suggesting the presence of glyphosate-tolerant EPSPS II pathway, whereas ASVs that decline in proportionate abundance will be more likely to exhibit proline in the codon 106 of the EPSPS gene, suggesting they possess the glyphosate-sensitive EPSPS class I. We further hypothesize that (iii) ASVs indicative of glyphosate exposure will also be more likely to possess the genes for C-P lyase as this would enable them to take full advantage of their glyphosate tolerance by breaking down glyphosate to bioavailable phosphate.

Chapter 2

Methods

234   2.1 Methods

235   Biofilm communities are complex and varied and extremely difficult to culture. To conduct

236   controlled experiments to produce environmentally relevant results, we used artificial substrates

237   deployed in natural lacustrine and riverine wetlands on which biofilm communities assembled during

238   a minimum four-week incubation period. These communities were then transferred to laboratory

239   microcosms to conduct the experiments. The experiment was carried out twice: once in 2018 using

240   biofilms collected from marshes next to tributary mouths (riverine wetlands) (Figure 1) and again in

241   2019 using biofilms from a combination of riverine wetlands and lacustrine wetland (marshes further

242   from water flow) stations (Figure 1). Additional differences in methods between the 2018 and 2019

243   trials are summarized below and detailed in Appendix D.

244
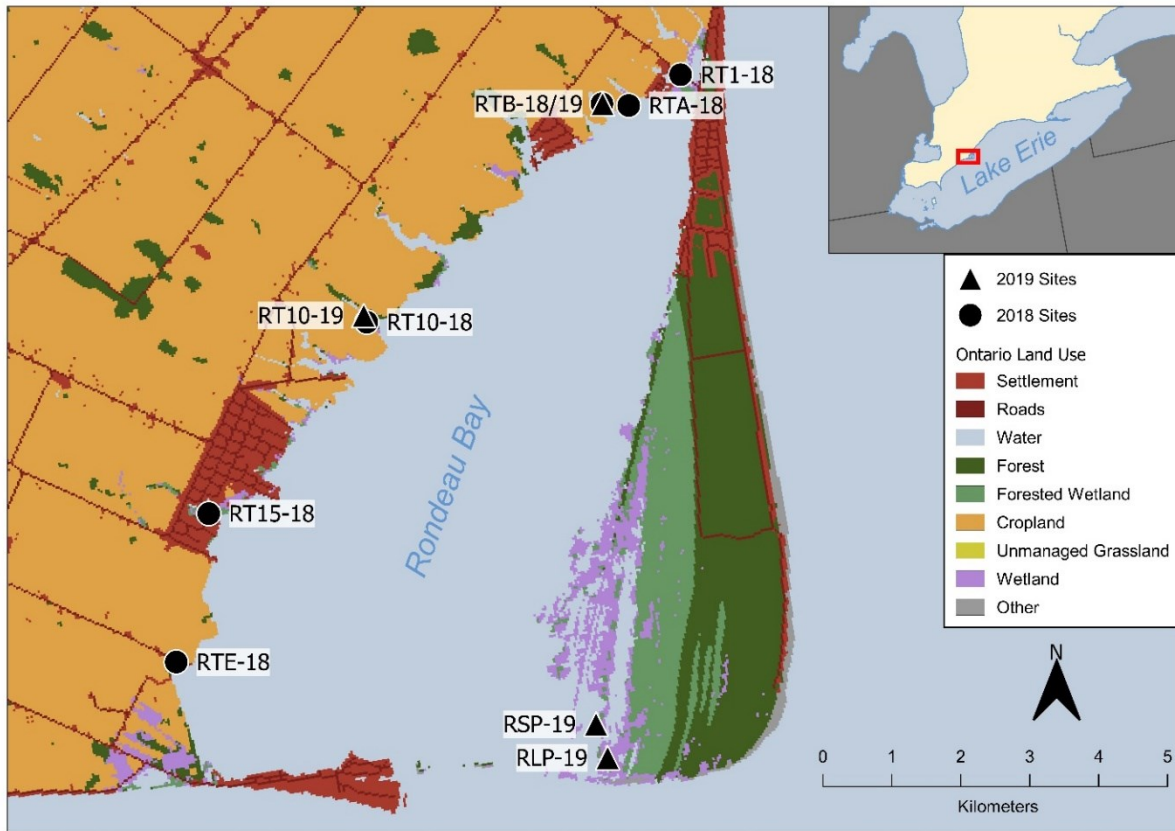
Figure 1: Map of *in situ* colonization sites around Rondeau Bay on the north shore of Lake Erie. Circles indicate sites that were sampled in 2018 while triangles indicate sites that were sampled in 2019. This map was created using QGIS with land cover derived from the 2018 Agriculture and Agri-Food Canada Annual Crop Inventory (AAFC, 2019) and the inset used in a QGIS base layer with data originating from Statistics Canada 2011 Census and the United States Census Bureau 2019; EPSG: 3347, using the NAD83 / Statistics Canada Lambert Projection.

2.2 *In situ* Biofilm Colonization

Biofilms were cultured on artificial substrates consisting of plexiglass plates (approximately 44.6 cm x 20.2 cm x 0.7 cm). We suspended the plates from rope by gill net buoys so that they were 10 cm below the surface of the water and held in place by rebar and T poles to form arrays (Figure 2). Arrays were situated in shallow water, between approximately 50 and 100 cm in depth. Artificial substrates were then left to colonize and equilibrate for a minimum of four weeks for biofilm colonization before collection to ensure complete colonization (Chaumet et al., 2020).

10

259   In 2018, we installed the arrays on May 23 and 24 at six riverine wetland sites in tributaries

260   of Rondeau Bay on the north shore of Lake Erie (Figure 1), with five plates per site. We collected the

261   arrays in two batches. We collected the first batch from the wetlands on August 27, 2018 and

262   transferred the plates to the culturing facility at the University of Waterloo in the Department of

263   Biology. The second batch remained in the wetlands for the duration of the first glyphosate exposure

264   trial, and then were collected and transferred to the culturing facility on September 27, 2018, and the

265   exposure trial repeated.

266   In 2019, we installed the arrays in two riverine wetland sites and two lacustrine wetland sites

267   of Rondeau Bay (Figure 1) on June 12 with ten plates per site. We added lacustrine wetlands to

268   capture biofilms in sites experiencing less direct runoff from the agricultural lands that dominate the

269   Rondeau Bay catchment (Figure 1). These lacustrine wetlands were anticipated to support biofilms

270   relatively naïve to glyphosate, compared to the riverine wetland biofilms. We collected all the arrays

271   on July 18 and transferred them to the culturing facility at the University of Waterloo.
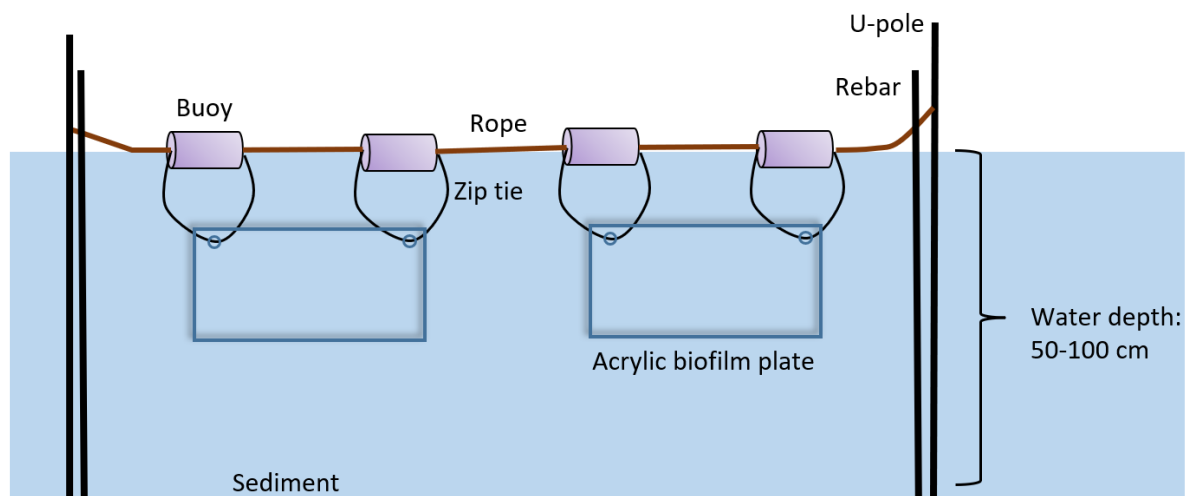
272

273   Figure 2: Diagram of biofilm collection array construction.

274   During collection, for both trials in 2018 and the single trial in 2019, we collected *in situ*

275   measurements of dissolved oxygen, conductivity, temperature, and pH; along with observations of

276   water depth, weather, and nearby vegetation. Dissolved oxygen and pH were collected with the Hach

277   HQ 30D flexi with Hach LDO and Hach IntelliCAL pH PHC201 attachments respectively (Hach:

278   London, Ontario); conductivity was collected with a dissolved solids tester (DiST) waterproof

279   EC/TDS °C/°F (Hanna: Woonsocket, Rhode Island). Temperature was measured with both devices to
280   give an average value. Plastic lined coolers filled with filtered lake water (100 μm Nitex) were used
281   to transport the plates back to the lab. During transport, the plates were held in place in coolers using
282   custom-made stands of high-density polyethylene (Science Technical Services Machine Shop,
283   University of Waterloo). As the plates were collected, a sterile cell scraper (Fisher Scientific, No. 08-
284   100240) was used to take a biofilm sample of an area approximately 1.9 cm x 20.2 cm for genetic
285   analysis. The collected biomass was placed in a Whirlpak bag with a small amount of deionized water
286   and stored in a Styrofoam cooler with an ice pack and was frozen when returned to the lab.

287   ## 2.3 Laboratory Microcosms

288   In the lab, we randomly assigned colonized plates to either a control microcosm with no
289   glyphosate exposure or a treatment microcosm with glyphosate exposure. There was a control and a
290   treatment microcosm for each site. Microcosms comprised 38 L glass aquaria lined with plastic bags
291   and filled with filtered lake water (100 μm Nitex) collected from Rondeau Provincial Park and
292   transported to the lab in carboys (Appendix A). Approximately 3-5 L of water was removed and
293   replaced with new filtered lake water every seventh day to refresh the microcosm water. Microcosms
294   were refilled to the original volume using markings on the tanks prior to each glyphosate addition to
295   replace loss from evaporation. The addition of water and occasional exchange were necessary to
296   prevent nutrient depletion and waste product accumulation, maintain consistent conditions and water
297   volumes (Figure 3). Since we are looking for the effects of glyphosate on biofilm community
298   structure, and also for the potential breakdown of glyphosate to AMPA and eventually phosphorus
299   through C-P lyase, we did not provide any additional nutrient supplementation (Sviridov et al., 2015).
300   We relied instead on the regular replenishing of lake water to sufficiently prevent nutrient depletion,
301   without over supplying phosphorus sources outside of glyphosate.

302

303

304

305

306

12

Sample	*in situ*	Week 1	Week 2	Week 3	Week 4
Field Collection					
Glyphosate dose					
Glyphosate/AMPA sample					
Genetic sample					
Water condition measurements					
Water exchange					

Figure 3: Summary of experiment sampling schedule. Full list of samples is available in Appendix C.

The microcosms were equipped with air pumps and air diffusers to oxygenate and mix the water. Consistent conditions were confirmed by regular measurements of microcosm water (Table 1). Lithonia shop lights producing cool white light were set up with two 32 W T8 bulbs on a 14:10 h light:dark cycle under ambient lab temperature conditions. This range is comparable to natural light dark cycles in Southern Ontario during biofilm incubation.

Table 1: Mean and standard deviation of water conditions in microcosms for the duration of the experiments.

Condition Measurement	September 2018	October 2018	July 2019
Dissolved Oxygen (mg/L)	8.89 ($\pm$0.07)	8.84 ($\pm$0.42)	8.72 ($\pm$0.10)
Temperature (HACH LDO) (^{o}C)	20.6 ($\pm$0.20)	20.1 ($\pm$2.00)	21.6 ($\pm$0.90)
Conductivity (ppt)	0.12 ($\pm$0.01)	0.19 ($\pm$0.02)	0.14 ($\pm$0.02)
Temperature (DiST by HANNA) (^{o}C)	20.9 ($\pm$0.40)	20.3 ($\pm$2.10)	21.9 ($\pm$0.90)
pH	8.43 ($\pm$0.04)	8.47 ($\pm$0.09)	6.58 ($\pm$0.16)

2.4 Glyphosate Exposure and Sampling

We allowed the plates to rest undisturbed for at least two days to acclimatize to lab conditions before the glyphosate exposure experiment began. The exposure experiment and sample collection lasted 21 days.

13

321   We collected measurements every seventh day before we added glyphosate. These included
322   dissolved oxygen, pH, conductivity, and temperature. Prior to glyphosate addition, we collected a 100
323   mL water sample from each microcosm in acid washed polyethylene sample bottles. The sample
324   bottles were pre-rinsed with sample water and then samples were frozen until analysis for glyphosate
325   and AMPA concentrations (Figure 3). Tanks were refilled with filtered lake water prior to glyphosate
326   addition to ensure accurate concentrations. Every 3.5 days, 0.5 mg glyphosate a.e./L from a 480 mg/L
327   stock solution of glyphosate (RoundUp Custom, made from the isopropylamine salt form of
328   glyphosate (CAS 38641-94-0), manufactured by U.S. Bayer Corporation; Whippany, New Jersey)
329   was added to the treatment microcosms (Appendix D). This concentration was chosen to be an
330   environmentally relevant level based on glyphosate monitoring data compiled in a review by Annett
331   et al., (2014). It is a plausible environmental concentration for agriculturally impacted areas, that is
332   also high enough to potentially influence biofilm communities. We chose to dose biweekly to
333   simulate pulse-exposure that may be seen in agricultural runoff; specifically, the regular, but not
334   continuous exposure due to indirect glyphosate use (Boxall et al., 2002; Chow et al., 2020).

335   On every seventh day, we collected biofilm samples for genetic analysis from each
336   microcosm using the same sterile cell scraper method described above.

2.5 Chemical Analyses

338   Glyphosate and AMPA concentrations in microcosm water samples were analyzed by the
339   Agriculture and Food Laboratory (AFL) at the University of Guelph. Samples were first
340   homogenized, fortified with internal standard and then centrifuged. The supernatant was then
341   acidified prior to liquid chromatography and mass spectrometry, and the samples quantified using a
342   ratio of external to internal standard. The limits of detection and quantification varied by analyte and
343   sample matrix and are listed in Table 2.

344

345

346

347 Table 2: Limits of Detection (LOD) and Limits of Quantification (LOQ) for glyphosate and AMPA
348 analysis from AFL.

Analyte	Sample Matrix	LOD (ppm)	LOQ (ppm)
Glyphosate	Water	0.001	0.008
Glyphosate	Biofilm	0.005	0.02
AMPA	Water	0.002	0.008
AMPA	Biofilm	0.005	0.02

349

2.6 Bioinformatics

351   Genetic analysis was completed by MetagenomBio Inc. using Illumina sequencing (Illumina
352 MiSeq v2 kit for paired end read lengths of 250 bp). The bacteria and archaea component of the
353 community (16S rRNA) was analyzed using a 16S universal V4 region primer
354 (dx.doi.org/10.1128/mSystems.00009-15). Frozen samples were submitted to MetagenomBio Inc. on
355 February 11, 2019 and October 11, 2019. The marker gene sequences were converted to a sample-
356 wise abundance table with sequence-based amplified sequence variants (ASVs). These sequences
357 were assigned preliminary taxonomy by MetagenomBio Inc. based on reference databases (e.g.,
358 SILVA). Demultiplexed sequences were processed using DADA2 v1.8 (Callahan et al., 2016)
359 managed through QIIME 2 v.2019.7 (https://qiime2.org/, Caporaso et al., 2010). In this workflow
360 forward and reverse reads were truncated at decreasing quality (typically ca. 225 forward and 175
361 reverse), primers were removed, and paired reads were assembled after Illumina sequencing error
362 modelling and correction. Subsequently, chimeric ASVs were removed by reconstruction against
363 more abundant parent ASVs. An ASV table was then constructed for downstream analysis.
364 Taxonomy was assigned to representative sequences using a naive Bayesian classifier implemented in
365 QIIME 2 with scikit-learn (v.0.20.3) trained against SILVA release 132 clustered at 99% identity.
366 Assignments were accepted above a 0.7 confidence threshold. Assigned taxonomy was used
367 exclusively for exploratory analyses, including the QIIME frequency chart (Section 3.2-3.3). All
368 following analyses were carried out on the ASV proportionate reads within a sample (i.e., the ASV
369 count as a proportion of the total counts within the sample) because the raw ASV counts are
370 dependent upon the success of the primer for the individual samples. Additionally, different
371 organisms may contain multiple copies of the amplified sequence in their genome, such that they

372 appear more abundant in terms of raw counts. To prevent this "double counting," values must be
373 standardized to proportionate reads prior to analysis.

374 Next, we investigated the subset of ASVs that differed in their proportionate reads between
375 the control and treatment samples to determine whether they possessed certain proteins that are
376 known to confer resistance to glyphosate; specifically, a mutant version of the EPSPS enzyme and C-
377 P lyase. The subset of ASVs were identified to a closest matching known organism through the
378 National Centre for Biotechnology Information's (NCBI) Basic Local Alignment Search Tool
379 (BLAST) using a nucleotide>nucleotide search (https://blast.ncbi.nlm.nih.gov/Blast.cgi). Criteria for
380 a match was a percent identity >97%, an E value $<1*10^{-6}$, and a representative genome available in
381 the NCBI database. A representative genome was required to have a >97% percent identity and
382 $<1*10^{-6}$ E value to the candidate match. This subset of ASVs that did not have a representative
383 genome match with a percent identity >97%, an E value $<1*10^{-6}$ were identified to the phylum level
384 using their closest known match determined during the initial BLAST. The phylum identity was
385 determined using the NCBI Taxonomy Browser (Sayers et al., 2019; Schoch et al., 2020).

386 We then performed a protein>protein BLAST search to compare the representative genomes
387 with a known class I proline EPSPS enzyme (Appendix I; Appendix J). This was done to determine
388 whether the EPSPS class was a factor in the indicator species reaction to treatment group. The
389 representative genomes were also run with a protein>protein BLAST search with a representative *E.*
390 *coli phnJ* gene (https://www.ncbi.nlm.nih.gov/nuccore/NC_000913.3?report=fasta; Appendix I;
391 Appendix J) to determine if indicator species possibly contained functional C-P lyase pathways.
392 Representative genomes with a matching *E. coli phnJ* gene were also matched to other *phn* genes to
393 determine likelihood of functional C-P lyase. Both protein>protein BLASTs with the EPSPS enzyme
394 and the *phn* genes required an E value $<1*10^{-6}$.

2.7 Statistical Analysis

396 Richness (S) and Shannon-Weiner Diversity (H') were calculated after rarefying samples to a
397 common library size (Cameron et al., 2021; Schmidt et al., 2021). Rarefying and diversity
398 calculations were completed through RStudio v. 1.3.1073 using code adapted from Cameron et al.,
399 2021. The minimum library size used in rarefying was 2717, however the rarefy curve (Figure 4)
400 demonstrated that most samples would not be adequately captured at the minimum size, so an
401 additional library size of 10,000 was included in the analysis. While the 10,000 library size will more

402   adequately capture the range of most samples, this will also remove samples where the library size

403   was below 10,000; therefore, richness and diversity were calculated for both library sizes (Table 3).
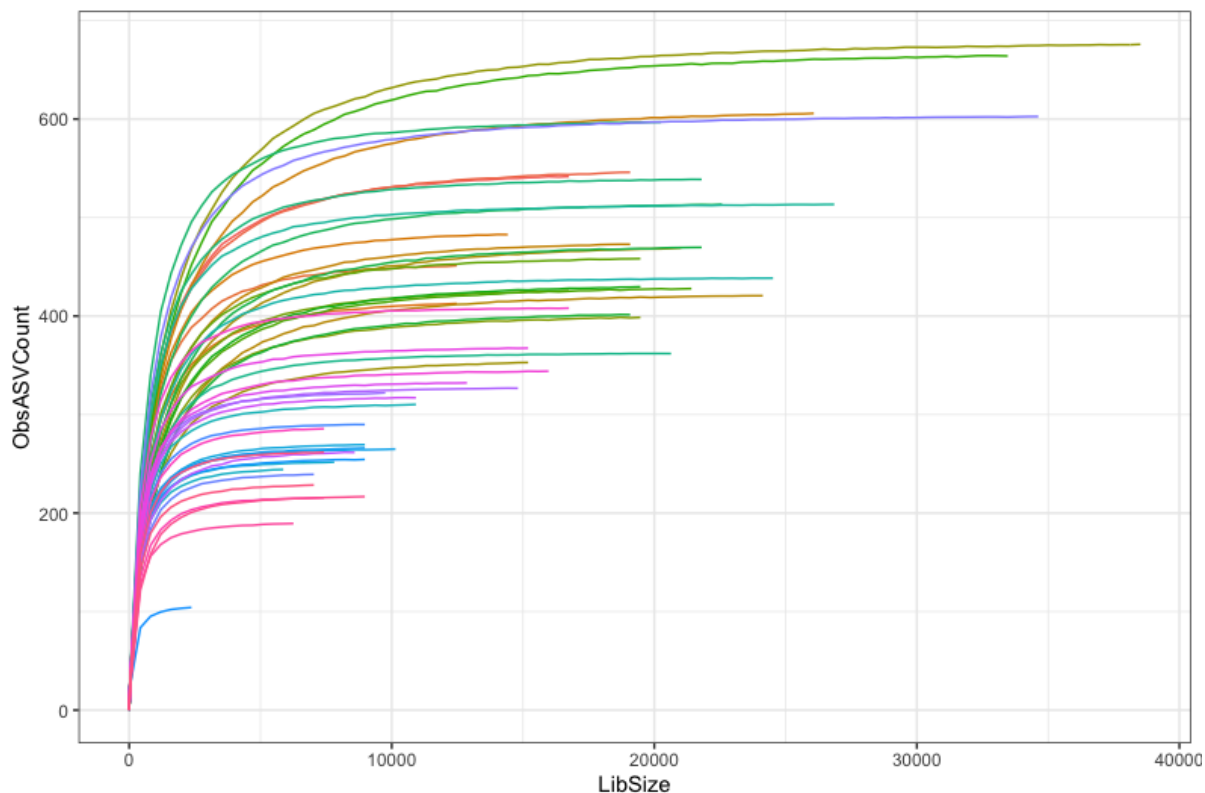
404

405   Figure 4: Rarefy curve from RStudio. The minimum library size recommended based on the curve is

406   2717; however, the curve adequately captures most samples at a library size >10,000.

407   We tested whether the diversity of bacteria and archaea differed between the control and

408   treatment microcosms by two-way ANOVAs with fixed factors to test effect of treatment (control and

409   treatment), date (experiment day one and experiment day 21), and the interaction of these factors;

410   with normality assumptions tested with an Anderson-Darling test. The two-way ANOVAs were

411   performed with type III sums of squares and was completed using Systat v. 13.2 (Systat Software Inc,

412   2017). The two-factor ANOVA was performed twice, with the first analysis on all samples (n = 40)

413   and the second analysis on only the riverine samples (n = 36).

414   In preliminary analyses, we found the composition of biofilms from the two lacustrine

415   wetland sites sampled in 2019 was so distinct from the composition of biofilms from the riverine

416   wetlands sampled in 2018 and 2019 that it obscured possible differences between control and

417   treatment samples (Figures 5 and 6). Therefore, we excluded the lacustrine sites from the multivariate

418   analyses of bacteria and archaea community composition.

419   We analyzed the bacteria and archaea ASV data using PC-ORD v7.01 (McCune & Mefford,

420   2015). Data returned by MetagenomBio Inc. is raw counts of ASVs from each sample. These counts

421   are dependent on the success of a primer and the number of times the target sequence appears in a

422   genome; therefore, the samples must be relativized before comparing sites. The counts were first

423   relativized to each ASV as a proportion of the sample total. The proportions were then transformed

424   using an arc-sine square-root transformation, as recommended for compositional data (McCune &

425   Grace, 2002):

426
$$b = \left(\frac{2}{\pi}\right) \arcsin\left(\sqrt{x_{ij}}\right)$$

427   We performed a non-metric multidimensional scaling ordination (NMS) on samples from the

428   first and final day of the in-lab portion of the experiment from riverine wetlands to visualize the

429   hypothesis that biofilm community composition would differ between the control and treatment

430   microcosms over time (n = 32 samples; distance measure = Bray-Curtis). We assessed dimensionality

431   using a chance corrected evaluation approach comparing the lowest final stress with average stress

432   from 250 random starting configurations, with the coordinates assigned as uniform random variables.

433   This tested the null model that the final configuration was no improvement over the initial random

434   configuration. We report the stress of the final solution and its nonmetric fit.

435   We performed a randomized complete block permutational multivariate analysis of variance

436   (RCB PerMANOVA) using the Bray-Curtis distance measure to test the hypothesis that biofilm

437   community composition would differ significantly between the control and treatment samples. To

438   control for site-to-site variation, the riverine wetland number was used as a blocking variable,

439   separated by year, with treatment as the fixed factor. The analysis was focused on the final day of the

440   experiment (day 21) and restricted to samples from 2018 and 2019 riverine wetlands (n = 16

441   samples).

442   We performed a blocked indicator species analysis (blocked ISA) to determine if any specific

443   ASVs were driving change in biofilm community composition, again with a Bray-Curtis distance

444   measure. As in the RCB PerMANOVA analysis, we used riverine wetland site number as a blocking

445   variable, separated by year, and treatment type (control vs. treatment) as the grouping variable (n = 16

18

446   samples). We considered the full list of ASVs detected in samples from day 21 and designated

447   significant indicators of either the treatment or control groups using an alpha of 0.1 because of the

448   relatively small sample size (n = 16), compared to the more than 2000 ASVs detected from the day 21

449   samples.

450

451

Chapter 3

Results

3.1 Experimental Conditions

Glyphosate and AMPA were not detected *in situ* for the riverine wetland samples collected in 2018, but both glyphosate and AMPA were found in low concentrations in both riverine and wetland site when biofilm samples were collected in 2019 (≤ 0.025 mg a.e./L glyphosate; ≤ 0.004 mg a.e./L AMPA) (Appendix K). Glyphosate and AMPA concentrations in treatment microcosms increased over the course of the 21-day experiment (Figure 5). A single dose of glyphosate was mistakenly added to the control microcosm for site RLP on day 3, but otherwise glyphosate and AMPA were not detected in the control microcosms. A maximum glyphosate concentration of 1.8 mg a.e./L was found in the RTA treatment microcosm on day 21, while a maximum AMPA concentration of 1.1 mg a.e./L was found in the RT10 (2019) treatment microcosm on day 14.

RTA   RTB (2018)

RTE   RT1

RT10 (2018)   RT15

RTB (2019)   RT10 (2019)

*RLP   RSP

Glyphosate Concentration (mg a.e./L)

AMPA Concentration (mg a.e./L)

Experiment Day

464
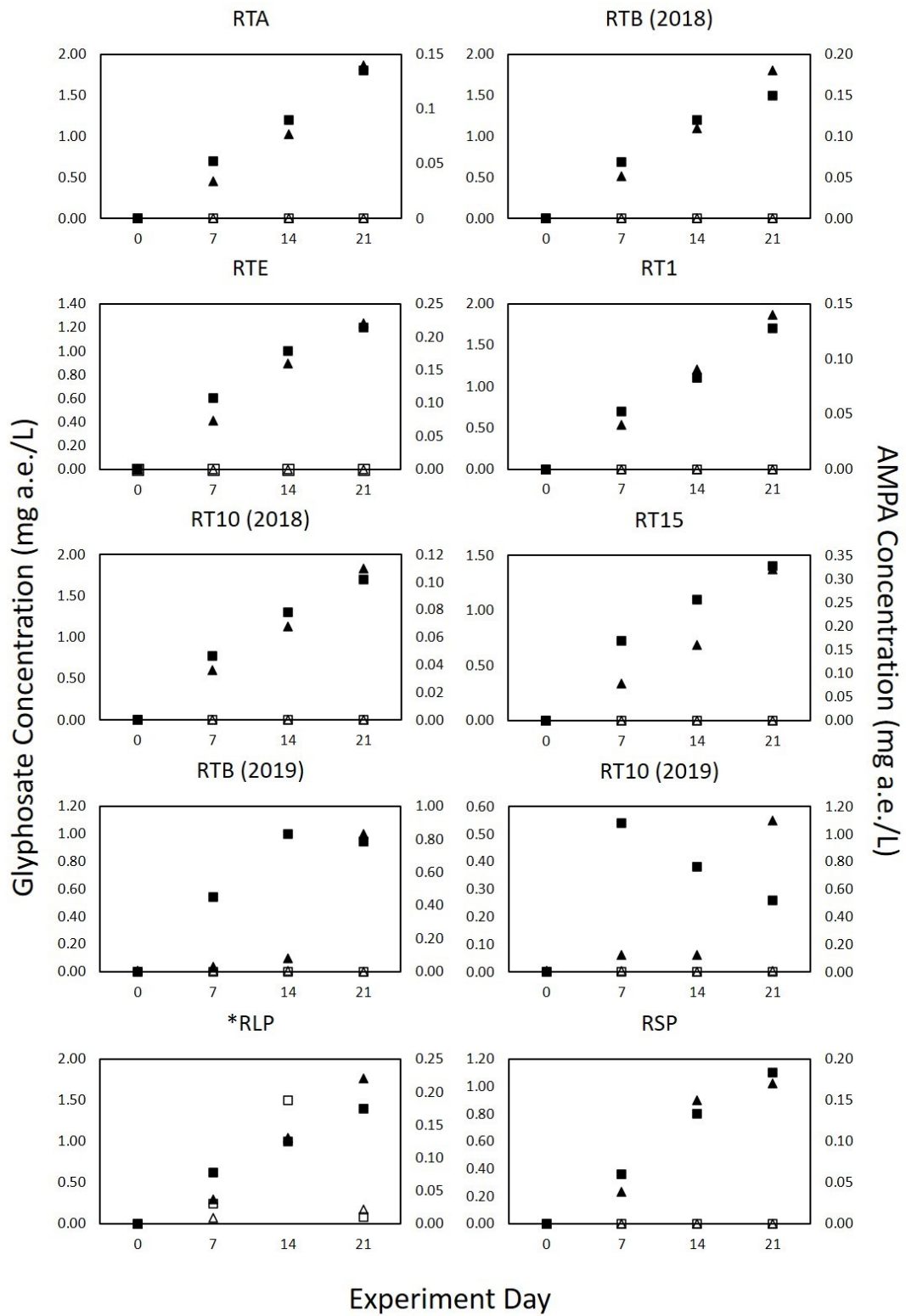
465 Figure 5: Glyphosate (squares) and AMPA (triangles) concentrations measured in control (empty
466 symbols) and treatment (filled symbols) in microcosms over the 21-day exposure experiment. *One
467 glyphosate dose was mistakenly added to RLP microcosm on day 3.

3.2 Results of Amplification and Sequencing

469   Unfiltered ASV data is available at DOI: 10.6084/m9.figshare.16987873. The average count
470 across all samples was 23,144 with a standard deviation of 11,417.3. There was a maximum count of
471 56,791 in the 2019 *in situ* sample from RT10 and there was a minimum count of 4232 in the day 21
472 control sample from RT15 in 2018. Prior to denoising, sequence depth ranged from 4232 to 56,791
473 (Appendix G). After denoising, sequence depth ranged from 2717 to 38,863 (Appendix G).

3.3 Summary of Filtered and Rarefied ASV Data

475   After quality control by MetagenomBio Inc., 5883 distinct ASVs (average length of 253 +/-
476 2.35 bp) were identified across all samples from both years, though not all these were detected from
477 the biofilm samples collected *in situ* (3001 ASVs in total; Table 3). There was taxonomic turnover
478 between the control and treatment biofilm samples and over time between the first and 21st day of the
479 experiment (Table 3; Figure 6).

480   The biofilm communities were found to contain both bacteria and archaea. The bacteria were
481 diverse, containing more than a dozen phyla, but were heavily dominated by Proteobacteria.
482 Cyanobacteria were relatively uncommon in samples collected *in situ*, but their relative abundance
483 increased under laboratory conditions, making them the second most abundant bacterial phylum. The
484 gains in relative abundance of cyanobacterial ASVs was slightly greater in control than treatment
485 microcosms, but was evident in both microcosm types. Other abundant phyla included Bacteroidetes,
486 Planctomycetes, Chloroflexi, and Acidobacteria. Verrucomicrobia, though their relative abundance
487 decreased under laboratory conditions compared to *in situ* (Figure 6). Archaea, by contrast were
488 relatively rare in the biofilms and were restricted to the Nanoarchaeota and Thaumarchaeota phyla
489 (Figure 6). Of the 5883 ASVs identified, 129 were only able to be identified to Bacteria in the initial
490 taxonomic assignation based on Silva databases, suggesting that they were previously undescribed.
491 (Figure 6: Legend 14).

492

493 Table 3: ASV summary for bacteria and archaea across all sites following quality control and rarefying. *In situ* samples were collected when plates

494 were collected from the field. Day 1 samples were collected on the first day of the experiment and Day 21 samples were collected on the final day

495 of the experiment. ASV summary includes the cumulative number of ASVs identified across each category, the mean and standard deviation

496 (StDev) of the rarefied ASV count and diversity index results for both the 2717 and 10,000 library sizes. Full summary of rarefied richness and

497 diversity calculations is available in Appendix G.

	Cumulative ASVs identified per treatment x date	Mean ASV Count per site (Library 2717)	StDev ASV Count per site (Library 2717)	Mean ASV Count per site (Library 10,000)	StDev ASV Count per site (Library 10,000)	Mean Diversity Index per site (Library 2717)	StDev Diversity Index per site (Library 2717)	Mean Diversity Index per site (Library 10,000)	StDev Diversity Index per site (Library 10,000)
Control Day 1	2271	329.912	89.781	436.449	82.338	5.039	0.379	5.223	0.372
Control Day 21	1936	292.115	85.999	388.487	46.065	4.654	0.565	4.894	0.513
Treatment Day 1	2328	332.369	73.739	451.366	35.937	5.030	0.275	5.213	0.296
Treatment Day 21	2076	318.757	69.811	397.752	88.168	4.935	0.266	5.018	0.321
In situ	3001	395.951	115.565	527.653	130.259	5.242	0.350	5.437	0.278

498

499

500

501

502
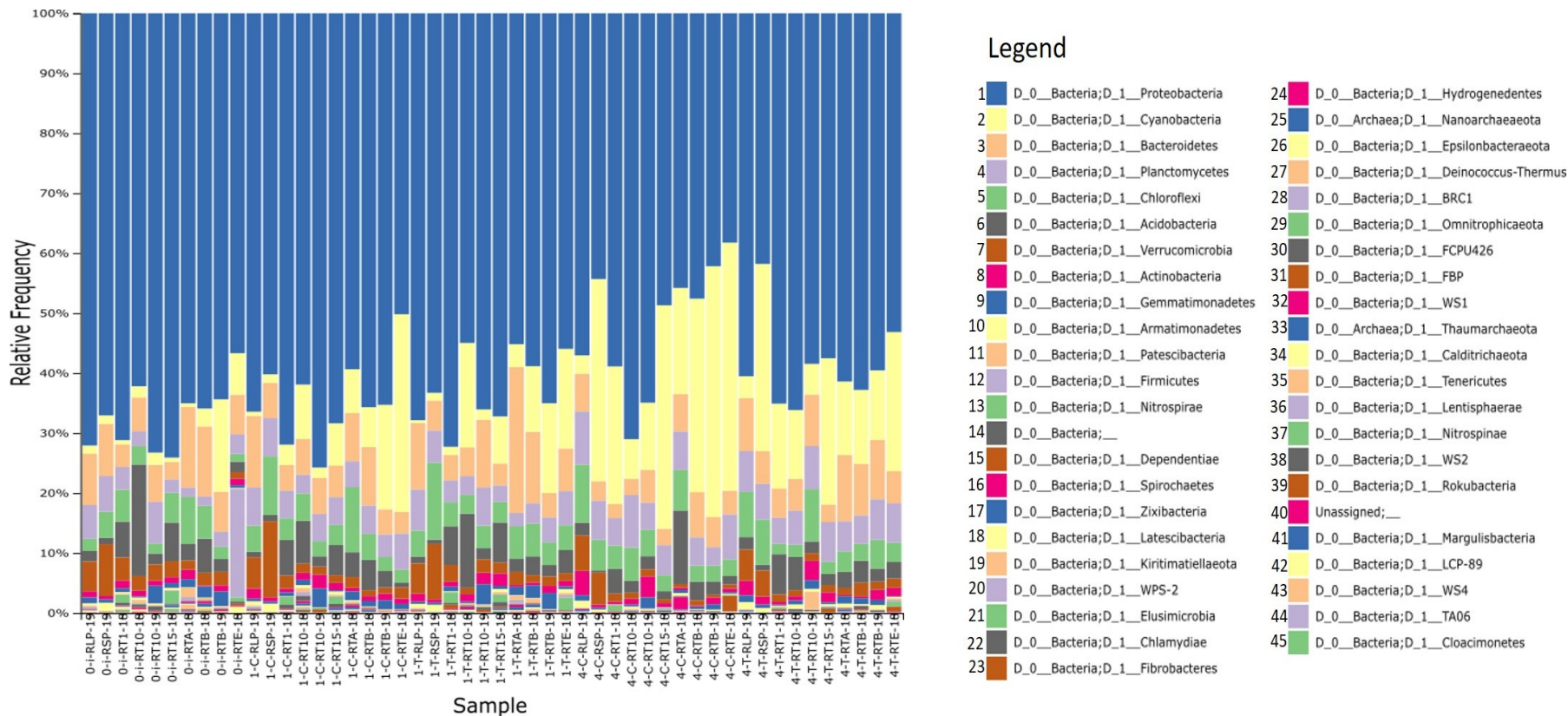
Figure 6: QIIME relative frequency chart showing ASVs found in all samples at the phyla level (level 2). Site codes (x axis) indicate 0-I for *in situ*

samples; 1 for samples taken on the first day of the experiment and 4 for samples taken on the final day of the experiment; C indicates control

samples while T indicates treatment samples; next is the site code; the final number is the year. The legend indicates phylum level identification

for both bacteria and archaea.

3.4 Diversity Analysis Results

The result of the two-way ANOVA found that there was no significant effect of treatment or date on richness or Shannon-Weiner diversity for all samples or the subset of riverine samples, and there was no significant interaction of the two factors on richness or diversity for all samples or the subset of riverine samples (Table 4). Full results of the Two-Way ANOVA and plots of Least Squared Means are available in Appendix G.

Table 4: Results of two-way ANOVA on richness (S) and Shannon-Weiner diversity (H') for both the 2717 and the 10,000 library sizes. Calculations were done for all samples and for a subset of riverine samples.

Dataset	Library Size	Analysis	Factor	Degrees of Freedom	F-Value	p-Value	R^2
All Samples	2717	S	Treatment	1,36	0.329	0.570	0.042
			Date	1,36	1.026	0.318	0.042
			Treatment*Date	1,36	0.227	0.637	0.042
		H'	Treatment	1,36	1.210	0.279	0.150
			Date	1,36	3.785	0.060	0.150
			Treatment*Date	1,36	1.381	0.248	0.150
	10,000	S	Treatment	1,23	0.212	0.649	0.145
			Date	1,23	3.743	0.065	0.145
			Treatment*Date	1,23	0.012	0.915	0.145
		H'	Treatment	1,23	0.147	0.705	0.130
			Date	1,23	3.066	0.093	0.130
			Treatment*Date	1,23	0.203	0.657	0.130
Riverine Samples	2717	S	Treatment	1,32	1.814	0.187	0.079
			Date	1,32	0.847	0.364	0.079
			Treatment*Date	1,32	0.158	0.693	0.079
		H'	Treatment	1,32	2.372	0.133	0.173
			Date	1,32	3.508	0.070	0.173
			Treatment*Date	1,32	1.223	0.277	0.173
	10,000	S	Treatment	1,19	1.523	0.232	0.183
			Date	1,19	2.679	0.118	0.183
			Treatment*Date	1,19	0.074	0.788	0.183
		H'	Treatment	1,19	0.337	0.568	0.123
			Date	1,19	2.365	0.141	0.123
			Treatment*Date	1,19	0.073	0.789	0.123

3.5 Dendrogram and NMS Figures

The last join in the dendrogram combined the lacustrine samples with the riverine samples at 0.0% information remaining (distance = 9.669), indicating that they were the most distinctive groups of samples (Figure 7). Within the riverine and lacustrine branches, samples from the same site showed high degrees of similarity in ASV proportionate reads, clustering together between 46.9% information remaining (site RT15) and 80.3% information remaining (site RSP). However, sites showed high interannual variation. The two riverine wetlands sampled in 2018 and 2019 clustered more closely with sites sampled in the same year than with the samples collected from the same site in different years: both RT10 and RTB sampled in 2018 merged with the 2019 samples at about 10% information remaining. This supports using site*year as a blocking variable in other analyses. With the exception of the 2019 samples from RTA and RTE, dissimilarity in biofilm ASV composition was lower between control and treatment samples from the same site*year than between samples at the start (day 1) and end of the exposure experiment (day 21). However, the degree of dissimilarity in ASV composition tended to be higher between control and treatment microcosms sampled at the end of the experimental period than at the beginning of the exposure experiment.

532
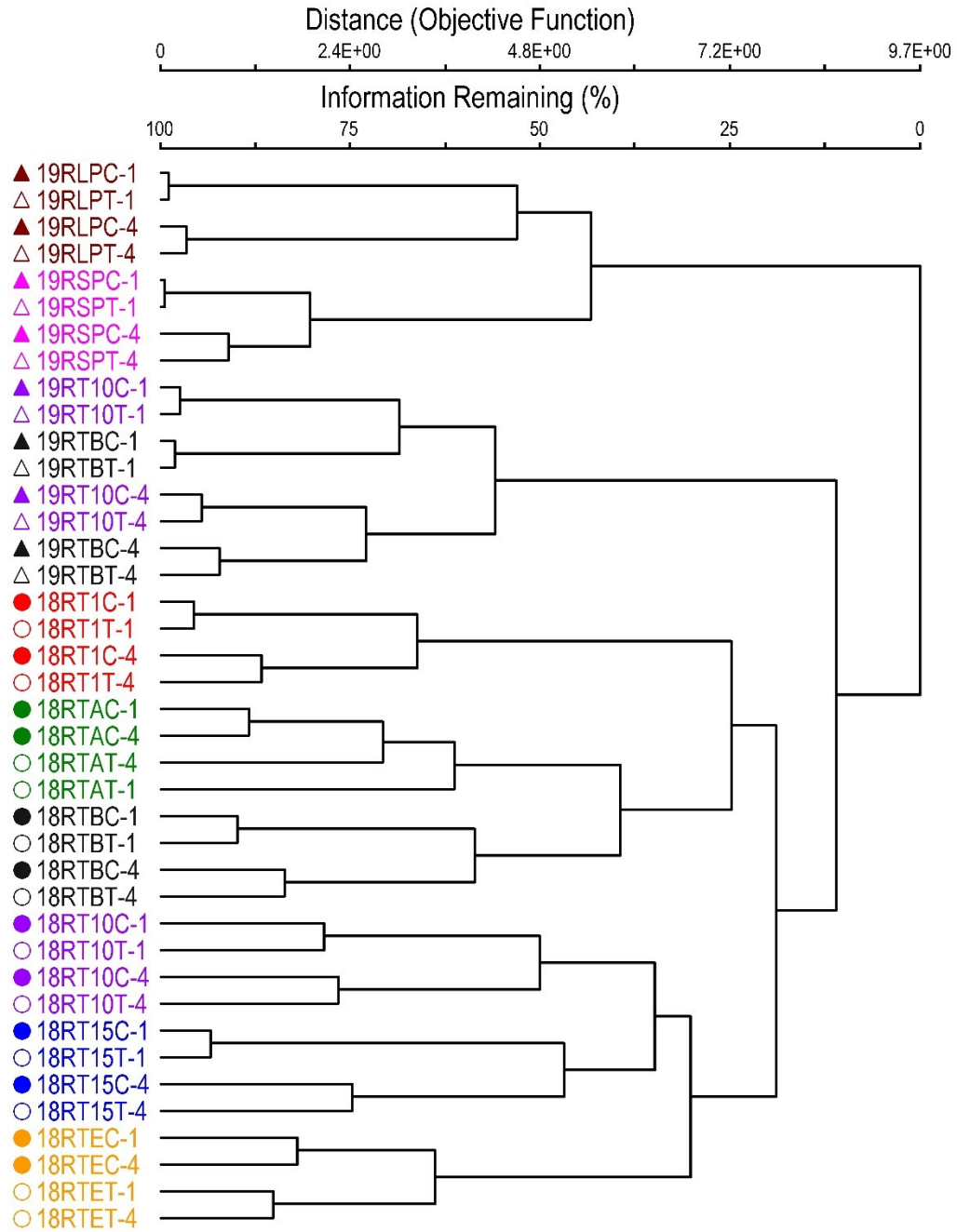
Figure 7: This dendrogram of riverine and lacustrine wetland sites demonstrates a separation of the

riverine wetland samples (bottom 32 samples) from the lacustrine wetland samples (top 8 samples).

Samples tend to relate the most to samples from the same site except for RTB and RT10 which are

mixed together. Filled symbols indicate treatment samples while open symbols indicate control

537   samples. Sites are separated by text colour and are labeled with site codes (e.g., RLP). The first

538   number in the sample code indicates the year the sample was taken; along with circles indicating

539   2018 samples, and triangles indicating 2019 samples. The final number of the sample code indicates

540   the sample date with -1 indicating samples taken on day 1 of the exposure experiment and -4

541   indicating samples taken on day 21 of the exposure experiment.

542

543   The optimal NMS solution including both riverine and lacustrine wetlands had three

544   dimensions, which collectively explained 77.2% of the variance in the Bray-Curtis dissimilarity

545   matrix of arcsine square-root transformed proportionate ASV reads. The first axis explained 48.5%,

546   the second 17.5%, and the third 11.2%. This final solution had a stress of 10.86 and a stability of

547   <0.0001, achieved after 103 iterations (Chance-corrected evaluation I = 0.6851, A = 0.3900; non-

548   metric R^2 = 0.9882) (Figure 8).
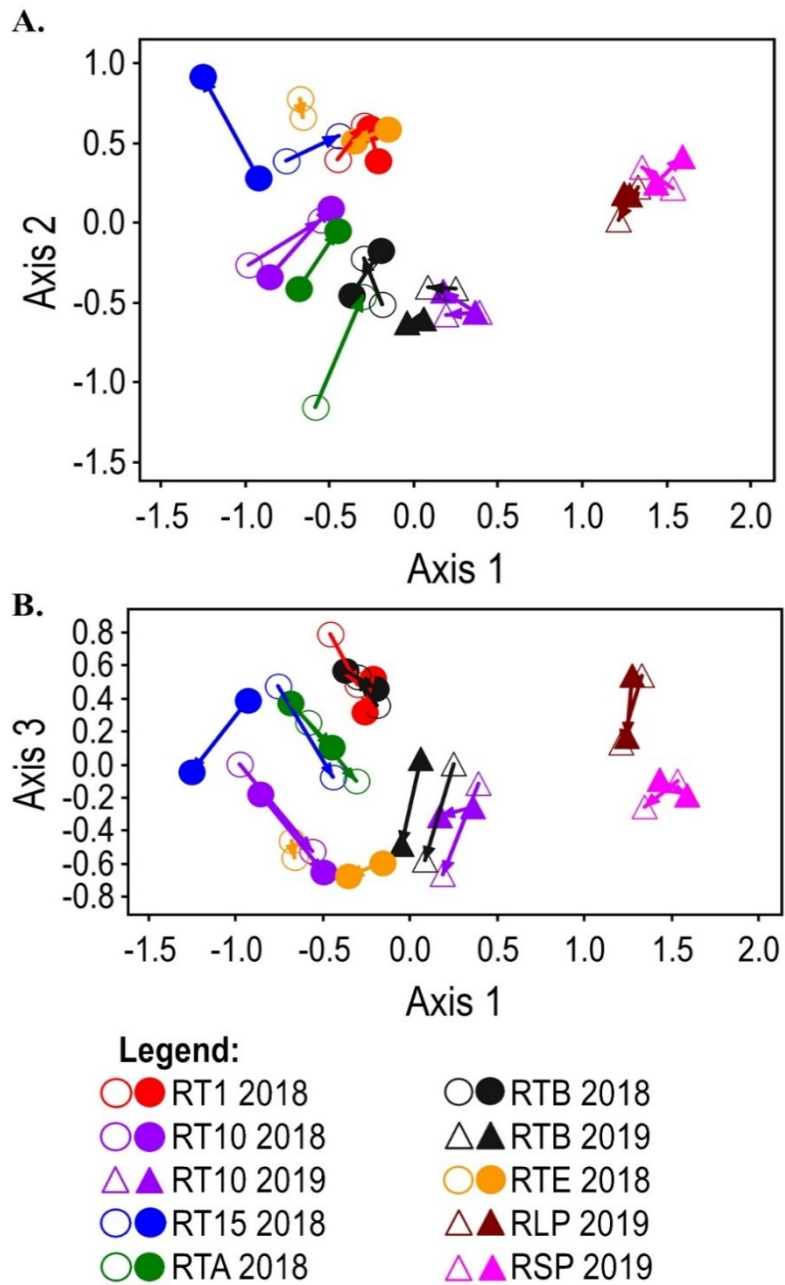
Figure 8: Three-dimensional Nonmetric Multidimensional Scaling visualization for the bacteria and archaea component of the biofilm community for all riverine and lacustrine wetland sites sampled in 2018 (circles) and 2019 (triangles), with symbol colour differentiating the sites and symbol fill

553   differentiating treatment microcosms (hollow) and control microcosms (filled). The vectors extend

554   from the start of the experiment (day 1 microcosm samples) to the end of the experiment (day 21

555   microcosm samples). Panel A depicts axes 1 and 2, whereas panel B depicts axis 1 and 3.

556

557   Substantiating the results of the cluster analysis, the lacustrine and riverine wetland sites

558   showed the greatest divergence in ASV composition (Figure 8), segregating on axis 1. In contrast, the

559   differences between control and treatment biofilm samples from the same sites on the same dates

560   were minor. Therefore, NMS and additional multivariate analyses were run on only the riverine

561   wetland biofilms to better resolve the effects of glyphosate exposure from the inherent differences

562   between riverine and lacustrine wetland types.

563   Considering only the biofilm communities collected from riverine wetlands, the optimal

564   NMS solution also had three dimensions, which collectively explained 76.3% of the variance in the

565   Bray-Curtis dissimilarity matrix of arcsine square-root transformed proportionate ASV reads. The fist

566   axis explained 42.6%, the second 17.8%, and the third 15.9%. This final solution had a stress of 11.72

567   and a stability of <0.0001, achieved after 56 iterations (Chance-corrected evaluations: I = 0.6585, A =

568   0.3390; non-metric R^2 = 0.9863) (Figure 9). Generally, there were clear succession effects evident on

569   axis 2, with day 1 samples having higher axis 2 scores than day 21 samples, regardless of site, year, or

570   treatment.

571

572
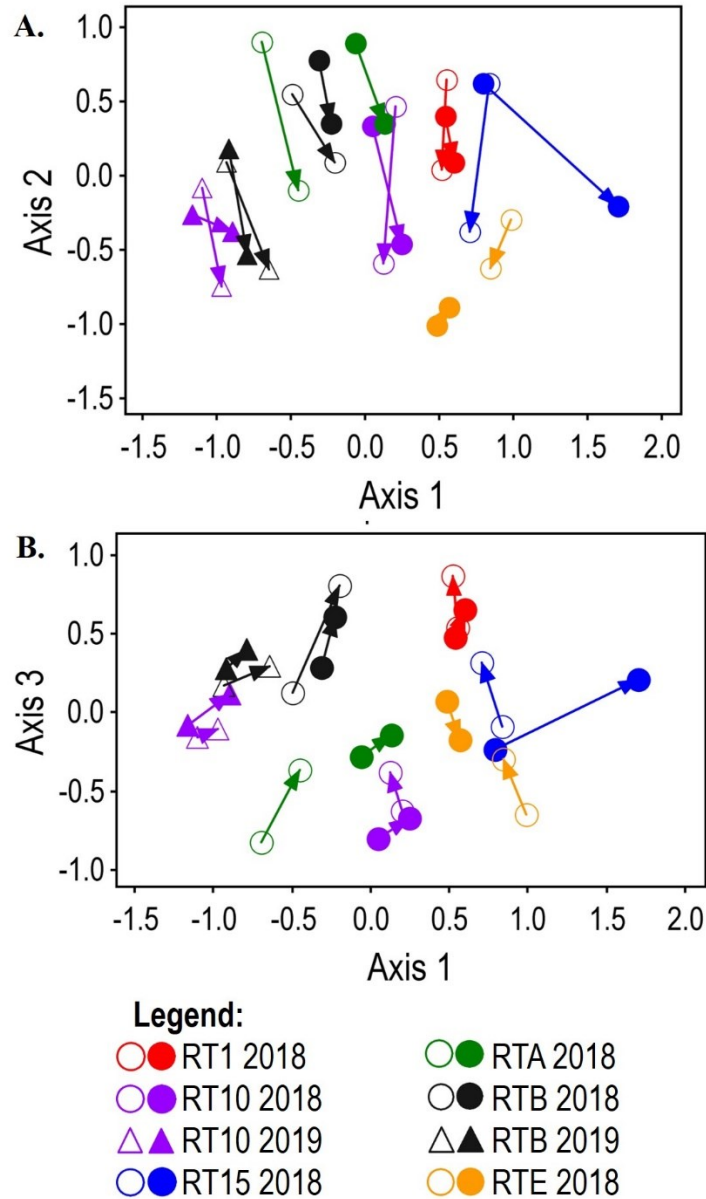
Figure 9: Three-dimensional Nonmetric Multidimensional Scaling visualization for the bacteria and archaea component of the biofilm community for only riverine wetland sites. Symbol colour differentiates the six riverine wetland sites, symbol shape differentiates 2018 (circles) from 2019 (triangles) experimental exposures, and symbol fill distinguishes treatment (hollow) from control (filled) microcosms. The vectors extend from the start of the experiment (day 1 microcosm samples)

578 to the end of the experiment (day 21 microcosm samples). Panel A depicts axes 1 vs 2, whereas panel
579 B depicts axes 1 vs 3.

580

3.6 Randomized Complete Block PerMANOVA Results

582 While statistically controlling for site*year as a blocking variable, there was a significant
583 effect of treatment on the bacteria and archaea community composition, based on the proportionate
584 reads among ASVs (Table 5).

585 Table 5: Results of the randomized complete block PerMANOVA analysis of bacteria and archaea
586 proportionate reads among riverine wetland samples, with site*year as a blocking variable and
587 treatment as fixed factor.

Source	d.f.	SS	MS	F	p-value*	Variance component (%)
Year*site (blocking variable)	7	2.9518	0.42169	4.5999	0.000200	72.065
Treatment	1	0.18325	0.18325	1.9989	0.008600	Not estimated for fixed factor
Residual	7	0.64172	0.09167			27.935
Total	15	3.7768				100

588 *p-values represent the proportion of 49,999 randomized trials where the F value exceeded the
589 observed F value.

590

3.7 Blocked ISA Results

592 Eight ASVs were indicative of control microcosms and 20 ASVs were indicative of treatment
593 microcosms at a p-value <0.1 (Table 6).

594

32

Table 6: Summary of indicator species with p < 0.1. ID codes indicate which ASV is considered an indicator. Full sequences are available in supplementary material (Appendix H) for indicator species that appeared in any samples from the final day of the experiment, and these can be identified using the ID Code.

| ID Code | Treatment Group | Observed Indicator Value (IV) | Indicator Value from randomized groups | | p-value |
			Mean	Standard Deviation	
BPlan508	Control	63	47.9	8.69	0.0152
BProt2050	Control	72.3	44.9	11.4	0.0316
BProt2789	Treatment	77.3	43.7	11.54	0.0318
BCyan297	Control	58.3	42.3	8.58	0.0320
BBact105	Treatment	66.2	54.1	8.71	0.0468
BProt2245	Treatment	52	43.7	4.96	0.0582
BProt563	Treatment	56.3	31.5	11.93	0.0590
BProt2251	Treatment	58.1	41.3	8.6	0.0594
BProt539	Treatment	62.5	30.2	11.37	0.0598
BProt2279	Treatment	62.5	30.5	11.41	0.0602
BVerr64	Treatment	53.2	34.9	8.96	0.0602
BProt2361	Control	62.5	30.5	11.42	0.0604
BProt2172	Control	57	31.9	11.77	0.0608
BProt2157	Treatment	42.2	37.5	2.39	0.0610
BPlan518	Treatment	64.2	47.6	8.6	0.0612
BProt616	Treatment	54.4	35	9.11	0.0618
BVerr258	Treatment	51.1	35.1	8.75	0.0628
BProt2208	Control	58.1	32.2	11.72	0.0636
BProt2051	Control	48.9	35.3	8.64	0.0636
BProt2788	Treatment	62.5	30.7	11.63	0.0654
BAcid72	Treatment	42.1	37.5	2.52	0.0668
BPlan367	Control	65.4	54.3	8.69	0.0706
BProt2189	Treatment	62.9	47.6	8.54	0.0916
BProt425	Treatment	59.6	56.2	2.46	0.0936

| ID Code | Treatment Group | Observed Indicator Value (IV) | Indicator Value from randomized groups | | p-value |
			Mean	Standard Deviation	
BProt153	Treatment	56.7	41.5	8.74	0.0940
BGemm35	Treatment	61.7	38.4	11.75	0.0950
BPlan313	Treatment	39.8	38.6	0.94	0.0960
BCyan307	Treatment	60.7	38.4	11.64	0.0978

599

3.8 Indicator ASV Phylum Identification

601   Of the 28 indicator ASVs identified, only ten had representative genomes available on the

602   NCBI Nucleotide Collection. All indicator ASVs were identified to phylum level based on the closest

603   matching species identified through the nucleotide->nucleotide BLAST (Table 7). More than half of

604   the indicators from both control and treatment microcosms are from the phylum Proteobacteria.

605   Planctomycetes and Cyanobacteria were also indicators in both control and treatment microcosms.

606   Treatment microcosms had distinct indicators of Gemmatimonadetes, Bacteroidetes, Acidobacteria,

607   and Verrucomicrobia (Table 7).

608

609   Table 7: Summary of the most likely phylum candidate for all 28 indicator ASVs. The phylum

610   candidate is the phylum of the closest relative identified in the initial nucleotide->nucleotide BLAST.

611   Further detail of the BLAST results can be found in Appendix J.

ID Code	Treatment Group	Closest BLAST Species Identified	E Value	Percent Identity	Phylum Candidate
BProt2172	Control	*Hydrogenophaga luteola*	5.00E-142	100	Proteobacteria
BPlan508	Control	*Planctopirus hydrillae*	4.00E-78	90.16	Planctomycetes
BProt2361	Control	*Sulfuritortus calidifontis*	9.00E-104	93.68	Proteobacteria
BPlan367	Control	*Blastopirellula marina*	1.00E-84	90.51	Planctomycetes
BProt2208	Control	*Rhizobacter profundi*	1.00E-139	99.6	Proteobacteria
BProt2051	Control	*Acidovorax valerianellae*	1.00E-139	99.6	Proteobacteria
BCyan297	Control	*Cronbergia siamensis*	2.00E-55	85.71	Cyanobacteria
BProt2050	Control	*Piscinibacter aquaticus*	1.00E-139	99.6	Proteobacteria
BGemm35	Treatment	*Gemmatimonas phototrophica*	1.00E-96	92.77	Gemmatimonadetes
BProt425	Treatment	*Hyphomicrobium aestuarii*	3.00E-137	99.21	Proteobacteria

ID Code	Treatment Group	Closest BLAST Species Identified	E Value	Percent Identity	Phylum Candidate
BProt539	Treatment	*Phreatobacter stygius*	1.00E-108	94.47	Proteobacteria
BBact105	Treatment	*Terrimonas lutea*	2.00E-132	98.42	Bacteroidetes
BAcid72	Treatment	*Stenotrophobacter terrae*	5.00E-99	92.89	Acidobacteria
BProt2251	Treatment	*Methylophilus methylotrophs*	3.00E-137	99.21	Proteobacteria
BProt2157	Treatment	*Azohydromonas lata*	5.00E-142	100	Proteobacteria
BProt2189	Treatment	*Herminiimonas aquatilis*	7.00E-123	96.84	Proteobacteria
BProt563	Treatment	*Xanthobacter tagetidis*	2.00E-101	93.28	Proteobacteria
BVerr258	Treatment	*Prosthecobacter fusiformis*	6.00E-80	89.33	Verrucomicrobia
BProt616	Treatment	*Gemmobacter lanyuensis*	5.00E-142	100	Proteobacteria
BProt2788	Treatment	*Pseudomonas aeruginosa*	3.00E-137	99.21	Proteobacteria
BProt153	Treatment	*Aetherobacter rufus*	7.00E-123	96.84	Proteobacteria
BPlan518	Treatment	*Planctopirus hydrillae*	3.00E-66	88.19	Planctomycetes
BProt2279	Treatment	*Viridibacterium curvum*	5.00E-99	92.89	Proteobacteria
BProt2789	Treatment	*Pseudomonas fulva*	5.00E-142	100	Proteobacteria
BVerr64	Treatment	*Oleiharenicola alkatitolerans*	2.00E-120	96.44	Verrucomicrobia
BCyan307	Treatment	*Neosynechococcus sphagnicola*	5.00E-96	92.46	Cyanobacteria
BPlan313	Treatment	*Blastopirellula retiformator*	6.00E-71	88.84	Planctomycetes
BProt2245	Treatment	*Rivicola pingtungensis*	4.00E-118	96.05	Proteobacteria

612

3.9 EPSPS Protein Results and Figures

613

614   Of the 28 indicator ASVs identified, four indicator ASVs diagnostic of control microcosms

615 and six indicator ASVs diagnostic of treatment microcosms had representative genomes on the NCBI

616 Nucleotide Collection (Appendix J) to be analyzed via protein BLAST. All indicator ASVs diagnostic

617 of the control microcosms with representative genomes on the NCBI non-redundant protein

618 sequences database were found to have proline in the codon 106 position (Figure 10). Two indicator

619 ASVs diagnostic of the treatment microcosms with representative genomes also had proline in the

620 codon 106 position, while three indicator ASVs diagnostic of treatment microcosms were found to

621 have leucine in codon 106 (Table 8). There is also greater variety in the surrounding +/- four proteins

622 around codon 106 (Figure 10).

623

624

625   Table 8: Summary of EPSPS protein BLAST completed in August, 2020 of indicator ASVs when

626   compared to *E. coli* TAMRP. While 10 of the 28 indicator ASVs had an adequate genome match,

627   only eight of those representative genome matches adequately matched with a protein sequence.

628   Percent identity describes the match between the representative genome and the target protein

629   sequence (*E. coli* TAMRP). The E value is the likelihood of the protein sequence match occurring

630   due to random chance. The subject match is the portion of protein sequence including codon 106 that

631   are subject matches from the representative genome to the *E. coli* test sequence.

ID Code	Treatment Group	Representative Genome Match	Percent Identity	E Value	Subject Match
BProt2172	Control	*Hydrogenophaga flava* (taxid:65657)	53.09	3.00E-130	TAMRP
BProt2208	Control	*Rhizobacter gummiphilus* (taxid:946333)	53.03	2.00E-135	TAMRP
BProt2051	Control	*Acidovorax valerianellae* (taxid:187868)	54.18	4.00E-146	TAMRP
BProt2050	Control	*Piscinibacter aquaticus* (taxid:392597)	No significant similarity found		
BProt425	Treatment	*Hyphomicrobium nitrativorans* NL23 (taxid:1029756)	28.57	4.00E-34	TGARL
BProt2251	Treatment	*Methylophilus methylotrophus* (taxid:17)	54.31	6.00E-154	TAFRP
BProt2157	Treatment	*Azohydromonas lata* (taxid:45677)	51.34	4.00E-132	TAMRP
BProt616	Treatment	*Gemmobacter aquatilis* (taxid:933059)	29.02	9.00E-35	TGVRL
BProt2788	Treatment	*Pseudomonas aeruginosa* PAO1 (taxid:208964)	No significant similarity found		
BProt2789	Treatment	*Pseudomonas fulva* 12-X (taxid:743720)	28.81	3.00E-37	TSMRL

632

633
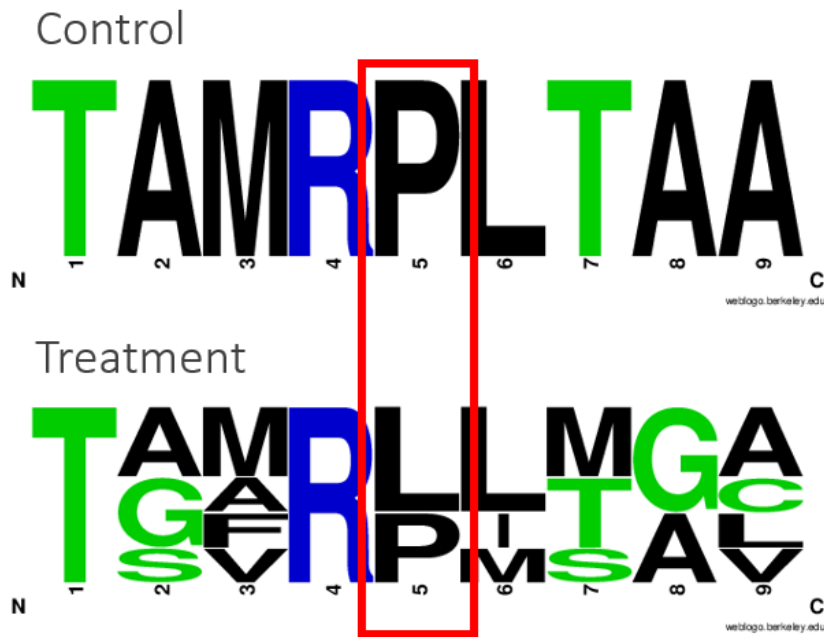
Figure 10: Frequency chart of codon 106 in control (n = 3) and treatment (n = 5) indicator species groups with eight nearest neighbour proteins. The ASVs indicative of control samples all had proline in codon 106 (position 5 in the frequency chart). The control samples indicator ASVs also had the same eight surrounding proteins. The treatment samples indicator ASVs had 60% leucine and 40% proline in codon 106 and also had a greater variety in surrounding proteins within the sequence.

639

3.10 C-P Lyase Results

Of the indicator species, 10 organisms were able to be identified in the NCBI Nucleotide Collection with a percent identity >97%. Eight of these species had a complete genome available to query in the NCBI non-redundant protein sequences database. When queried with the *phnJ* sample, three organisms were found to have significant similarity to the target sequence and were found to have a *phnJ* sequence in the genome (Table 9). These three were then tested against genes for each of the *phnCDEFGHIJKLMNP*. All three were found to have at least *phnGHIJK* which would suggest that these three organisms have functional C-P lyase (Table 9).

648 Table 9: Summary of C-P lyase protein BLAST of indicator species against E. coli *phn* genes. Of the
649 10 indicator species that had an adequate representative genome match, only three had adequate
650 sequence matches to the *phn* genes. Percent identity describes the match between the representative
651 genome and the target sequence (*phn* gene matches). The E value is the likelihood of the sequence
652 match occurring due to random chance. The *phn* match is confirmation of whether the representative
653 genome contained matching sequences of *phn* genes with significant similarity to the *E. coli*
654 comparison sequences. Most of the representative genomes did not have significant similarity with
655 any of the *phn* comparison genes.

| | | | | | *phn* gene match | | | | | | |
ID Code	Treatment Group	Representative Genome Match	Percent Identity	E Value	*phnG*	*phnH*	*phnI*	*phnJ*	*phnK*	*phnL*	*phnM*
BProt 2172	Control	*Hydrogenophaga flava* (taxid:65657)	No significant similarity.								
BProt 2208	Control	*Rhizobacter gummiphilus* (taxid:946333)	68.25	3.00E-143	Yes	Yes	Yes	Yes	Yes	Yes	Yes
BProt 2051	Control	*Acidovorax valerianellae* (taxid:187868)	No significant similarity.								
BProt 2050	Control	*Piscinibacter aquaticus* (taxid:392597)	No significant similarity.								
BProt 425	Treatment	*Hyphomicrobium nitrativorans* NL23 (taxid:1029756)	No significant similarity.								
BProt 2251	Treatment	*Methylophilus methylotrophus* (taxid:17)	No significant similarity.								

					phn gene match							
ID Code	**Treatment Group**	**Representative Genome Match**	**Percent Identity**	**E Value**	*phnG*	*phnH*	*phnI*	*phnJ*	*phnK*	*phnL*	*phnM*
BProt 2157	Treatment	*Azohydromonas lata* (taxid:45677)	No significant similarity.								
BProt 616	Treatment	*Gemmobacter aquatilis* (taxid:933059)	No significant similarity.								
BProt 2788	Treatment	*Pseudomonas aeruginosa* PAO1 (taxid:208964)	71.74	1.00E-153	Yes	Yes	Yes	Yes	Yes	Yes	Yes
BProt 2789	Treatment	*Pseudomonas fulva* 12-X (taxid:743720)	77.54	2.00E-168	Yes	Yes	Yes	Yes	Yes	Yes	Yes

656

657

Chapter 4

Discussion

660   Biofilms are extremely diverse communities that perform important ecological functions;

661   supporting food chains and cycling nutrients in a wide variety of aquatic ecosystems (Battin et al.,

662   2016; Flemming & Wuertz, 2019; Pérez et al., 2011; Wu, 2017). The diversity in these communities

663   is driven by both biotic and abiotic factors (Larned, 2010), including the influence of anthropogenic

664   factors such as nutrients and pesticides (Beecraft & Rooney, 2020; Hove-Jensen et al., 2014; Sviridov

665   et al., 2015). Glyphosate is one of the most commonly used herbicides in the world, and has been

666   detected in surface waters across North America and globally (Maggi et al., 2020; Medalie et al.,

667   2020), leading to numerous studies on its potential effects on aquatic organisms and systems (e.g.

668   Annett et al., 2014). The response of a biofilm community to glyphosate exposure is influenced by a

669   number of factors including the community composition, with glyphosate-tolerant organisms likely

670   outlasting glyphosate-sensitive organisms (Pollegioni et al., 2011). The EPSPS enzymatic pathway is

671   one way to determine glyphosate response (Pollegioni et al., 2011). The objective of this study was to

672   determine if pure glyphosate affected the bacteria and archaea community composition within

673   freshwater biofilms following a 21-day pulse exposure experiment and to test for the presence of

674   genetic sequences within indicative communities that would confer glyphosate resistance and/or the

675   ability to use glyphosate as a phosphorus source.

676   Our microcosm communities were largely dominated by Proteobacteria, although the

677   photosynthetic Cyanobacteria increased in relative abundance in both control and treatment

678   microcosms from *in situ* levels. This may have been caused by lab conditions because the

679   microcosms were under direct light, while *in situ* conditions included shading from macrophytes

680   (Appendix A; Appendix B). However, the Cyanobacteria did not displace Proteobacteria to the same

681   degree in treatment microcosms as they did in control microcosms. This was unexpected as we had

682   hypothesized Cyanobacteria would respond favourably to treatment conditions due to their reported

683   tolerance of glyphosate exposure (Forlani et al., 2008; Powell et al., 1991). However, Proteobacteria

684   are also reported to tolerate glyphosate, and this may have allowed the Proteobacteria to maintain

685   their dominance in the treatment microcosms (Carles & Artigas, 2020). We also found that the

686   Verrucomicrobia generally declined in the experimental conditions compared to *in situ* which may be

687   due to its reported sensitivity to glyphosate in agricultural ecosystems (Allegrini et al., 2019).

688   Our microcosms also had small relative abundances of Archaea, specifically Nanoarchaeota

689   and Thaumarchaeota. Nanoarchaeota are obligate symbiont archaea with reduced genomes (Munson-

690   McGee et al., 2015). It is not clear from our sequencing approach which organism(s) it was symbiotic

691   with in our samples. It is known to associate with Crenarchaeota (Munson-McGee et al., 2015), a

692   phylum of archaea typical of anaerobic, high heat or low pH environments that we did not detect in

693   our samples. However, it has been identified as a dominant type of archaea in freshwater biofilms

694   collected from an experimental flume fed by White Clay Creek in southeastern Pennsylvania, USA

695   (Wang et al., 2020). Thaumarchaeota is a diverse phylum of ammonia-oxidizing archaea that are very

696   common in aquatic environments and are important for their nitrification function (Brochier-Armanet

697   et al., 2012) and their production of vitamin B12 (Doxey et al., 2015). Thaumarchaeota are reported

698   to occur in biofilms in a wide range of aquatic environments. For example, from chloraminated

699   drinking water distributions systems in the tropics (Cruz et al., 2020) to Icelandic hot springs

700   (Daebeler et al., 2018).

701   We hypothesized that there would be a difference between control and treatment microcosms

702   for bacteria and archaea in biofilm communities in terms of richness and diversity due to the known

703   effects of glyphosate on the EPSPS enzymatic pathway found within these organisms (Pollegioni et

704   al., 2011). Unexpectedly, the richness and diversity in these communities showed no significant

705   change based on estimates of ASV richness and Shannon-Wiener diversity index from sequenced

706   ASVs. This is similar to the results of Carles and Artigas (2020) that found no significant effect of

707   glyphosate on the richness or diversity of the bacterial component of freshwater biofilms when

708   simulating environmental exposure levels found in France (0.001-0.1- mg glyphosate a.e./L). When

709   studying the effects of glyphosate on bacterioplankton, Barbosa da Costa et al. (2020) found that their

710   highest dose (15 mg glyphosate a.e./L) had no effect on richness, but did result in lowering of the

711   Shannon-Weiner diversity. This supports our findings of freshwater bacteria being resilient to

712   environmentally realistic levels of glyphosate exposure, both within the protection of a biofilm, and

713   as planktonic bacteria.

714   We also hypothesized that there would be a difference between control and treatment

715   microcosms for bacteria and archaea in terms of community composition at the end of the 21-day

41

716   exposure. We anticipated observing a difference in glyphosate response between the riverine wetland

717   and lacustrine wetland sites, as we expected the lacustrine wetlands to have communities that were

718   more naïve to pesticide exposure. However, we observed that the initial differences in community

719   composition between the riverine wetlands and lacustrine wetlands was far greater than any

720   difference caused by glyphosate exposure (Figures 5 and 6). The differences between the riverine and

721   lacustrine communities may be driven by many environmental factors, including the degree of

722   macrophyte growth, nutrient loading, turbidity, and temperature (Battin et al., 2016). Glyphosate

723   exposure did not cause the lacustrine sites to become more similar to the riverine sites, suggesting that

724   the community differences between riverine and lacustrine biofilms was driven more by

725   environmental factors than by glyphosate exposure. This obscured any effect of glyphosate on

726   community composition when both lacustrine and riverine sites were included in a single NMS

727   ordination (Figure 9).

728   When only comparing the riverine wetland communities, however, we did find a significant

729   effect of glyphosate exposure on community composition over time (PerMANOVA). Both control

730   and treatment microcosms experienced a shift in community composition between day 1 and day 21,

731   but the microcosms treated with glyphosate experienced a greater change in composition than the

732   control microcosms (Figure 9). This contrasts with the bacterioplankton study conducted by Barbosa

733   da Costa et al. (2020) that found no significant effect of glyphosate at lower doses (0.3 mg glyphosate

734   a.e./L), but did find a significant effect at a high dose of glyphosate (15 mg glyphosate a.e./L). This

735   contrasts with our study where we would expect biofilms to be more resilient than plankton due to the

736   extracellular matrix. However, in our observations, we found that the communities exposed to

737   glyphosate did not noticeably become more similar in terms of the composition of ASVs in the

738   communities over the duration of the 21-day experiment (Figure 9). For example, the riverine wetland

739   sites on day 1 had an average Sorensen dissimilarity of 69.725, compared to day 21 with an average

740   Sorensen dissimilarity of 69.920. Thus, the glyphosate exposure did not have a homogenizing effect

741   on the biofilms. This suggests that other factors are maintaining pre-existing differences between

742   communities despite glyphosate exposure. Additional research could be conducted on the ability of

743   biofilms to recover from glyphosate exposure when returned to a natural environment, and whether or

744   not the exposed communities would return to community composition similar to their composition

745   before glyphosate exposure.

746   We found 28 ASVs indicative of treatment and control microcosms. Proteobacteria was the

747   dominant indicator ASV phylum in both control and treatment microcosms. Both control and

748   treatment microcosms also had indicator ASVs from Cyanobacteria and Planctomycetes. Only the

749   treatment microcosm had distinct indicators in the phyla Gemmatimonadetes, Bacteroidetes,

750   Acidobacteria, and Verrucomicrobia. This somewhat agrees with the findings by Carles et al., (2020)

751   which found Proteobacteria, Cyanobacteria, and Planctomycetes increased in relative abundance

752   when exposed to glyphosate, although they did find Bacteroidetes tended to be sensitive to glyphosate

753   exposure. This also contrasts with studies of microbes in agricultural soils, which found that

754   Acidobacteria (Newman et al., 2016) and Verrucomicrobia (Allegrini et al., 2019) decreased in

755   relative abundance when exposed to glyphosate. Gemmatimonadetes has been found to significantly

756   increase in abundance under glyphosate exposure in agricultural studies (Arango et al., 2014).

757   Although the phyla of Proteobacteria, Cyanobacteria, and Planctomycetes was shared between control

758   and treatment microcosms, the phyla estimate was often based on closest matches to different genera.

759   This suggests that while we can make some inferences about the community at a phylum level, there

760   is variation at lower taxonomic levels that is important to distinguish when looking for potential

761   indicator ASVs. With future genomic sequencing, we may be able to more accurately narrow our

762   indicator ASVs to specific genera or species that will provide specific organisms that may be used as

763   indicators of glyphosate exposure.

764   Based on our analysis of representative genomes, we infer that 60% of the ASVs indicating

765   glyphosate exposure possessed leucine in codon 106 of the EPSPS, and 100% of ASVs indicating the

766   control microcosms possessed proline in codon 106 (control n = 3; treatment n = 5; Figure 10; Table

767   8). While there were too few definitively identified ASVs to generalize from these results to all 28

768   indicator ASVs, this pattern supports our hypothesis that ASVs that increased in proportionate reads

769   when exposed to glyphosate most likely possessed the class II EPSPS enzymatic pathway. More

770   support of this interpretation is that the final glyphosate concentration was non-additive, being much

771   less than the total amount of glyphosate that we added. Additionally, the increasing concentrations of

772   AMPA measured in the microcosms over the experimental period confirms that microbial breakdown

773   of glyphosate was taking place in our microcosms. Mutations in codon 106 away from proline have

774   been shown to be related to glyphosate resistance in many vascular plant species as well (Alcántara-

775   De La Cruz et al., 2016; Karn & Jasieniuk, 2017). We observed that 30% of ASVs indicating

776   glyphosate exposure had proline in codon 106, indicating class I EPSPS. It is possible that other

777 factors conferring glyphosate tolerance that would allow some class I organisms to survive in
778 glyphosate exposed communities (Karn & Jasieniuk, 2017; Margaritopoulou et al., 2018; Tani et al.,
779 2015). These may include synchronization in the overexpression of EPSPS and ABC-transporter
780 genes (Alcántara-De La Cruz et al., 2016; Margaritopoulou et al., 2018; Tani et al., 2015) or other
781 alternative resistance mechanisms unrelated to EPSPS (Karn & Jasieniuk, 2017). Furthermore, the use
782 of representative genomes rather than fully sequenced environmental genomes requires reliance on
783 databases for sequence identification and indirect inference of traits rather than direct observation of
784 traits from our samples. Metagenomic sequencing or targeted sequencing of the EPSPS gene would
785 be valuable to confirm our inference that glyphosate exposed microbial communities have a higher
786 rate of EPSPS class II organisms. Further sequencing of genomes from natural biofilm communities
787 would also improve our ability to determine the significance of codon 106 mutations indicating
788 glyphosate exposure.

789 Finally, we found two ASVs that were indicative of glyphosate-exposed communities that
790 possessed potentially functional C-P lyase. This may support the theory that some glyphosate-tolerant
791 organisms may be able to use the breakdown products of glyphosate as a phosphorus source (Hove-
792 Jensen et al., 2014), however, limitations of natural communities being severely underrepresented in
793 genomic databases makes it impossible to say with certainty due to the low number of organisms
794 sufficiently identified. Further research into genomic sequencing of natural communities would
795 greatly improve our ability to study the roles of specific microorganisms in broader ecosystems
796 through gene sequences.

797 Some biofilms have also been shown to bioconcentrate glyphosate which would allow these
798 communities to function in a contaminant-removal role (Beecraft & Rooney, 2020). We observed that
799 glyphosate was broken down microbially by the biofilm within treatment microcosms as evidenced
800 by the increasing concentrations of AMPA over the duration of the experiment. This is similar to the
801 findings of Carles et al. (2019), who found riverine biofilms breaking down glyphosate into AMPA.
802 Additionally, a study done by Beecraft & Rooney (2020) found that biofilms specifically were driving
803 the breakdown of glyphosate to AMPA and subsequent release into the microcosm when compared to
804 identical microcosms with sterile plates. However, the long-term effects of community change on this
805 contaminant removal capacity are not well understood. Carles et al. (2019) did find that accumulation
806 of phosphorus through the breakdown of glyphosate had a negative effect on biofilms' degradation of
807 glyphosate. Future research should investigate the resilience and resistance of biofilm function to

808 chronic glyphosate exposure; as well as the ability of biofilm communities and specific ASVs to

809 recover from glyphosate exposure, similar to work by Barbosa da Costa et al., 2021 on

810 bacterioplankton.

811   The glyphosate exposure concentration used in this experiment was on the higher end of

812 realistic environmental exposure in North American aquatic ecosystems, but was much more realistic

813 than similar recent experiments (Barbosa da Costa et al., 2021). The effects of this exposure level

814 over an extended period were surprisingly minor. Due to the great difference in community

815 composition between riverine and lacustrine wetlands, our study focused on the riverine wetlands

816 where we had more sampling. However, the riverine sites may have already experienced some

817 glyphosate exposure from agricultural activity upstream and this may contribute to the low effect of

818 glyphosate that we observed. The variability between the biofilm communities, especially when

819 comparing riverine and lacustrine wetlands, highlights the heterogenous nature of biofilms that is

820 likely influenced by external environmental factors. Additionally, the transfer of field-cultured

821 biofilms to homogenized laboratory conditions changed the development of the biofilm communities

822 as evidenced by the change observed in the NMS for both control and treatment microcosms (Figure

823 9). With the inclusion of control microcosms along with the treatment microcosms, we were able to

824 determine that, while succession occurred due to homogenized conditions, the effect of glyphosate

825 exposure did significantly impact the community composition over time. While the community

826 composition of individual sites changed over time due to glyphosate exposure, the overall diversity

827 and richness of the community was not significantly affected. This tolerance suggests that freshwater

828 biofilms are relatively resilient to glyphosate exposures over extended time periods.

829   We also observed that there were some ASVs that appeared in lab samples that did not appear

830 in *in situ* samples. This variation may be due to the heterogenous nature of biofilm communities that

831 make it difficult to ensure consistency in sample composition. There is a possibility that these

832 previously unidentified ASVs were carried over from neighbouring microcosms or through the

833 replenishment of microcosms with filtered lake water. However, most ASVs identified in day 1 and

834 day 21 samples were also identified *in situ* and we are able to assume they are of wetland origin. Full

835 summary of ASVs identified in samples is available in Appendix F.

836   In the present study we used a prolonged exposure period of 21 days with regular pulses of

837 glyphosate and conducted an in-depth assessment of bacteria and archaea community composition

838   and protein sequences that both indicate and help to explain biofilm community response to

839   glyphosate exposure. It is important to note that the glyphosate used in our experiment did not include

840   any surfactants. While we were specifically looking at the effect of a commercial formulation of

841   glyphosate alone at a realistic concentration and in a realistic pulse-exposure experiment, the effect of

842   commercial formulations may differ from our observations if the commercial formulations include

843   other components like POEA surfactants, which are known to be highly toxic to aquatic life

844   (Mesnage et al., 2019; Rodriguez-Gil et al., 2016).

845   Ours study was in part limited by the lack of representative genomes of natural communities

846   available. Further genomic sequencing of diverse organisms would greatly benefit future research into

847   the effects of anthropogenic activities on specific organisms or specific enzymatic pathways within

848   natural communities. All sequences including our unknown sequences will all be deposited at DOI:

849   10.6084/m9.figshare.16987873. Future study may also focus on other aspects of biofilm communities

850   including algal composition, fungal composition, and other eukaryotic organisms that live among

851   biofilms. Additionally, further work may be done in the lacustrine wetlands to more clearly determine

852   the effects of glyphosate on more naïve ecosystems.

853

854 # Chapter 5

855 # Conclusions

856   Biweekly glyphosate loading over a 21-day period changed the bacteria and archaea
857 community composition within wetland biofilms, but it did not significantly change the richness or
858 Shannon-Weiner diversity of these microbial communities. The bacteria and archaea within biofilm
859 communities were more resilient to glyphosate exposure than we hypothesized, even at the higher end
860 of environmental exposure realistic in North American agricultural regions. Glyphosate was broken
861 down microbially by these wetland biofilms as observed by glyphosate concentrations reaching a
862 maximum of 1.8 mg glyphosate a.e. /L which is lower than the 6 x 0.5 mg glyphosate a.e. /L = 3 mg
863 glyphosate a.e./L added during the 21-day experiment, as well as increasing concentrations of the
864 glyphosate breakdown product AMPA (maximum of 1.1 mg glyphosate a.e. /L). Additionally, we
865 observed evidence that some species of bacteria within wetland biofilms may use glyphosate and its
866 breakdown products as a phosphorus source as two of the identifiable treatment indicator ASVs
867 contained *phn* genes associated with C-P lyase. However, there are many opportunities for further
868 research on freshwater biofilms to fully understand how glyphosate exposure and subsequent
869 community changes may alter the composition and structure of other microorganisms within biofilms,
870 such as algae and fungi. Further genomic sequencing of natural biofilm communities could also
871 greatly increase our understanding of the interactions between freshwater biofilms and anthropogenic
872 contaminants. Additionally, further study into the 28 indicator ASVs which changed most
873 dramatically in proportionate reads in response to glyphosate exposure may enhance monitoring
874 efforts to detect ephemeral glyphosate exposure in wetland ecosystems.

875

References

AAFC. (2019). 2018 Annual Crop Inventory. Ottawa, ON, Canada: Agriculture and Agri-Food Canada. Retrieved from https://open.canada.ca/data/en/dataset/ba2645d5-4458-414d-b196-6303ac06c1c9

Alcántara-De La Cruz, R., Rojano-Delgado, A. M., Giménez, M. J., Cruz-Hipolito, H. E., Domínguez-Valenzuela, J. A., Barro, F., & De Prado, R. (2016). First resistance mechanisms characterization in glyphosate-resistant Leptochloa virgata. *Frontiers in Plant Science*, *7*, 1–11. https://doi.org/10.3389/fpls.2016.01742

Allegrini, M., Gomez, E. del V., Smalla, K., & Zabaloy, M. C. (2019). Suppression treatment differentially influences the microbial community and the occurrence of broad host range plasmids in the rhizosphere of the model cover crop Avena sativa L. *PLoS ONE*, *14*(10), 1–29. https://doi.org/10.1371/journal.pone.0223600

Altschul, S. F., Gish, W., Miller, W., Myers, E. W., & Lipman, D. J. (1990). Basic local alignment search tool. *Journal of Molecular Biology*, *215*(3), 403–410. https://doi.org/10.1016/S0022-2836(05)80360-2

Annett, R., Habibi, H. R., & Hontela, A. (2014). Impact of glyphosate and glyphosate-based herbicides on the freshwater environment. *Journal of Applied Toxicology*, *34*(5), 458–479. https://doi.org/10.1002/jat.2997

Arango, L., Buddrus-Schiemann, K., Opelt, K., Lueders, T., Haesler, F., Schmid, M., … Hartmann, A. (2014). Effects of glyphosate on the bacterial community associated with roots of transgenic Roundup Ready® soybean. *European Journal of Soil Biology*, *63*, 41–48. https://doi.org/10.1016/j.ejsobi.2014.05.005

Barbosa da Costa, N., Fugère, V., Hébert, M. P., Xu, C. C. Y., Barrett, R. D. H., Beisner, B. E., … Shapiro, B. J. (2021). Resistance, resilience, and functional redundancy of freshwater bacterioplankton communities facing a gradient of agricultural stressors in a mesocosm experiment. *Molecular Ecology*, *30*(19), 4771–4788. https://doi.org/10.1111/mec.16100

Battaglin, W. A., Meyer, M. T., Kuivila, K. M., & Dietze, J. E. (2014). Glyphosate and its degradation product AMPA occur frequently and widely in U.S. soils, surface water, groundwater, and precipitation. *Journal of the American Water Resources Association*, *50*(2),

275–290. https://doi.org/10.1111/jawr.12159

Battin, T. J., Besemer, K., Bengtsson, M. M., Romani, A. M., & Packmann, A. I. (2016). The ecology and biogeochemistry of stream biofilms. *Nature Reviews Microbiology*, *14*(4), 251–263. https://doi.org/10.1038/nrmicro.2016.15

Beecraft, L., & Rooney, R. (2020). Bioconcentration of glyphosate in wetland biofilms. *Science of the Total Environment*, *756*. https://doi.org/10.1016/j.scitotenv.2020.143993

Benbrook, C. M. (2016). Trends in glyphosate herbicide use in the United States and globally. *Environmental Sciences Europe*, *28*(1), 1–15. https://doi.org/10.1186/s12302-016-0070-0

Boxall, A. B. A., Brown, C. D., & Barrett, K. L. (2002). Higher-tier laboratory methods for assessing the aquatic toxicity of pesticides. *Pest Management Science*, *58*(7), 637–648. https://doi.org/10.1002/ps.479

Breckels, R. D., & Kilgour, B. W. (2018). Aquatic herbicide applications for the control of aquatic plants in Canada : effects to nontarget aquatic organisms. *Environmental Reviews*, *6*(January), 1–6. https://doi.org/10.1016/j.aquaculture.2006.12.039

Brochier-Armanet, C., Gribaldo, S., & Forterre, P. (2012). Spotlight on the Thaumarchaeota. *ISME Journal*, *6*(2), 227–230. https://doi.org/10.1038/ismej.2011.145

Callahan, B. J., McMurdie, P. J., Rosen, M. J., Han, A. W., Johnson, A. J. A., & Holmes, S. P. (2016). DADA2: High-resolution sample inference from Illumina amplicon data. *Nature Methods*, *13*(7), 581–583. https://doi.org/10.1038/nmeth.3869

Cameron, E. S., Schmidt, P. J., Tremblay, B. J. M., Emelko, M. B., & Müller, K. M. (2021). Enhancing diversity analysis by repeatedly rarefying next generation sequencing data describing microbial communities. *Scientific Reports*, *11*(1), 1–13. https://doi.org/10.1038/s41598-021-01636-1

Caporaso, J. G., Kuczynski, J., Stombaugh, J., Bittinger, K., Bushman, F. D., Costello, E. K., … Knight, R. (2010). Correspondence: QIIME allows analysis of high- throughput community sequencing data. *Nature Publishing Group*, *7*(5), 335–336. https://doi.org/10.1038/nmeth0510-335

Carles, L., & Artigas, J. (2020). Interaction between glyphosate and dissolved phosphorus on

bacterial and eukaryotic communities from river biofilms. *Science of the Total Environment*, *719*, 137463. https://doi.org/10.1016/j.scitotenv.2020.137463

Carles, L., Gardon, H., Joseph, L., Sanchís, J., Farré, M., & Artigas, J. (2019). Meta-analysis of glyphosate contamination in surface waters and dissipation by biofilms. *Environment International*, *124*, 284–293. https://doi.org/10.1016/j.envint.2018.12.064

Chaumet, B., Mazzella, N., Neury-Ormanni, J., & Morin, S. (2020). Light and temperature influence on diuron bioaccumulation and toxicity in biofilms. *Ecotoxicology*, *29*(2), 185–195. https://doi.org/10.1007/s10646-020-02166-8

Chow, R., Scheidegger, R., Doppler, T., Dietzel, A., Fenicia, F., & Stamm, C. (2020). A review of long-term pesticide monitoring studies to assess surface water quality trends. *Water Research X*, *9*, 100064. https://doi.org/10.1016/j.wroa.2020.100064

Christy, S . L . , Karlander, E . P ., & Parochetti, J. V. (1981). Effects of Glyphosate on the Growth Rate of Chlorella. *Weed Science*, *29*(1), 5–7. Retrieved from https://www.jstor.org/stable/4043399

Cruz, M. C., Woo, Y., Flemming, H. C., & Wuertz, S. (2020). Nitrifying niche differentiation in biofilms from full-scale chloraminated drinking water distribution system. *Water Research*, *176*, 115738. https://doi.org/10.1016/j.watres.2020.115738

Daebeler, A., Herbold, C. W., Vierheilig, J., Sedlacek, C. J., Pjevac, P., Albertsen, M., … Wagner, M. (2018). Cultivation and genomic analysis of "Candidatus Nitrosocaldus islandicus," an obligately thermophilic, ammonia-oxidizing thaumarchaeon from a hot spring biofilm in Graendalur valley, Iceland. *Frontiers in Microbiology*, *9*(FEB), 1–16. https://doi.org/10.3389/fmicb.2018.00193

Doxey, A. C., Kurtz, D. A., Lynch, M. D. J., Sauder, L. A., & Neufeld, J. D. (2015). Aquatic metagenomes implicate Thaumarchaeota in global cobalamin production. *ISME Journal*, *9*(2), 461–471. https://doi.org/10.1038/ismej.2014.142

Farm and Food Care Ontario. (2015). Survey of Pesticide Use in Ontario, 2013/2014 Estimates of Pesticides Used on Field Crops and Fruit and Vegetable Crops. Retrieved from https://www.farmfoodcareon.org/wp-content/uploads/2016/10/ONTARIO-Pesticide-Use-Survey-Final-2013.pdf

Flemming, H. C., & Wuertz, S. (2019). Bacteria and archaea on Earth and their abundance in biofilms. *Nature Reviews Microbiology*, *17*(4), 247–260. https://doi.org/10.1038/s41579-019-0158-9

Forlani, G., Pavan, M., Gramek, M., Kafarski, P., & Lipok, J. (2008). Biochemical bases for a widespread tolerance of cyanobacteria to the phosphonate herbicide glyphosate. *Plant and Cell Physiology*, *49*(3), 443–456. https://doi.org/10.1093/pcp/pcn021

Gattás, F., Vinocur, A., Graziano, M., dos Santos Afonso, M., Pizarro, H., & Cataldo, D. (2016). Differential impact of Limnoperna fortunei-herbicide interaction between Roundup Max® and glyphosate on freshwater microscopic communities. *Environmental Science and Pollution Research*, *23*(18), 18869–18882. https://doi.org/10.1007/s11356-016-7005-6

Goldsborough, L. G., & Brown, D. J. (1988). Effect of glyphosate (Roundup® formulation) on periphytic algal photosynthesis. *Bulletin of Environmental Contamination and Toxicology*, *41*(2), 253–260. https://doi.org/10.1007/BF01705439

Hove-Jensen, B., Zechel, D. L., & Jochimsen, B. (2014). Utilization of Glyphosate as Phosphate Source: Biochemistry and Genetics of Bacterial Carbon-Phosphorus Lyase. *Microbiology and Molecular Biology Reviews*, *78*(1), 176–197. https://doi.org/10.1128/mmbr.00040-13

Karn, E., & Jasieniuk, M. (2017). Nucleotide diversity at site 106 of EPSPS in Lolium perenne L. ssp. multiflorum from california indicates multiple evolutionary origins of herbicide resistance. *Frontiers in Plant Science*, *8*(May), 1–9. https://doi.org/10.3389/fpls.2017.00777

Khadra, M., Planas, D., Girard, C., & Amyot, M. (2018). Age matters: Submersion period shapes community composition of lake biofilms under glyphosate stress. *Facets*, *3*(1), 934–951. https://doi.org/10.1139/facets-2018-0019

Kish, P. A. (2006). Evaluation of herbicide impact on periphyton community structure using the matlock periphytometer. *Journal of Freshwater Ecology*, *21*(2), 341–348. https://doi.org/10.1080/02705060.2006.9665004

Larned, S. T. (2010). A prospectus for periphyton: recent and future ecological research. *Journal of the North American Benthological Society*, *29*(1), 182–206. https://doi.org/10.1899/08-063.1

Lavoie, I., Vincent, W. F., Pienitz, R., & Painchaud, J. (2004). Benthic algae as bioindicators of agricultural pollution in the streams and rivers of southern Québec (Canada). *Aquatic Ecosystem*

Health and Management, *7*(1), 43–58. https://doi.org/10.1080/14634980490281236

Leino, L., Tall, T., Helander, M., Saloniemi, I., Saikkonen, K., Ruuskanen, S., & Puigbò, P. (2021). Classification of the glyphosate target enzyme (5-enolpyruvylshikimate-3-phosphate synthase) for assessing sensitivity of organisms to the herbicide. *Journal of Hazardous Materials*, *408*(August 2020), 1–8. https://doi.org/10.1016/j.jhazmat.2020.124556

Lozano, V. L., Vinocur, A., Sabio y García, C. A., Allende, L., Cristos, D. S., Rojas, D., … Pizarro, H. (2018). Effects of glyphosate and 2,4-D mixture on freshwater phytoplankton and periphyton communities: a microcosms approach. *Ecotoxicology and Environmental Safety*, *148*, 1010–1019. https://doi.org/10.1016/j.ecoenv.2017.12.006

Lu, H., Feng, Y., Wang, J., Wu, Y., Shao, H., & Yang, L. (2016). Responses of periphyton morphology, structure, and function to extreme nutrient loading. *Environmental Pollution*, *214*, 878–884. https://doi.org/10.1016/j.envpol.2016.03.069

Maggi, F., la Cecilia, D., Tang, F. H. M., & McBratney, A. (2020). The global environmental hazard of glyphosate use. *Science of the Total Environment*, *717*, 137167. https://doi.org/10.1016/j.scitotenv.2020.137167

Margaritopoulou, T., Tani, E., Chachalis, D., & Travlos, I. (2018). Involvement of epigenetic mechanisms in herbicide resistance: the case of conyza canadensis. *Agriculture (Switzerland)*, *8*(1), 1–9. https://doi.org/10.3390/agriculture8010017

McCune, B., & Mefford, M. J. (2015). PC-ORD Multivariate Analysis of Ecological Data. Gleneden Beach, Oregon, U.S.A: MjM Software.

McCune, B. P., & Grace, J. P. (2002). *Analysis of ecological communities*. *Journal of Experimental Marine Biology and Ecology* (Vol. 289). Gleneden Beach, Oregon, U.S.A: MjM Software Design. https://doi.org/10.1016/S0022-0981(03)00091-1

Medalie, L., Baker, N. T., Shoda, M. E., Stone, W. W., Meyer, M. T., Stets, E. G., & Wilson, M. (2020). Influence of land use and region on glyphosate and aminomethylphosphonic acid in streams in the USA. *Science of the Total Environment*, *707*, 136008. https://doi.org/10.1016/j.scitotenv.2019.136008

Mesnage, R., Benbrook, C., & Antoniou, M. N. (2019). Insight into the confusion over surfactant co-formulants in glyphosate-based herbicides. *Food and Chemical Toxicology*, *128*(March), 137–

145. https://doi.org/10.1016/j.fct.2019.03.053

Mesnage, R., Biserni, M., Wozniak, E., Xenakis, T., Mein, C. A., & Antoniou, M. N. (2018). Comparison of transcriptome responses to glyphosate, isoxaflutole, quizalofop-p-ethyl and mesotrione in the HepaRG cell line. *Toxicology Reports*, *5*(June), 819–826. https://doi.org/10.1016/j.toxrep.2018.08.005

Montuelle, B., Dorigo, U., Bérard, A., Volat, B., Bouchez, A., Tlili, A., … Pesce, S. (2010). The periphyton as a multimetric bioindicator for assessing the impact of land use on rivers: An overview of the Ardières-Morcille experimental watershed (France). *Hydrobiologia*, *657*(1), 123–141. https://doi.org/10.1007/s10750-010-0105-2

Moresco, C., & Rodrigues, L. (2014). Periphytic diatom as bioindicators in urban and rural streams. *Acta Scientiarum*, *36*(1), 67–78. https://doi.org/10.4025/actascibiolsci.v36i1.18175

Munson-McGee, J. H., Field, E. K., Bateson, M., Rooney, C., Stepanauskas, R., & Young, J. (2015). Distribution across Yellowstone National Park Hot Springs. *Applied and Environmental Microbiology*, *81*(22), 7860–7868. https://doi.org/10.1128/AEM.01539-15.Editor

Nandula, V. K., Montgomery, G. B., Vennapusa, A. R., Jugulam, M., Giacomini, D. A., Ray, J. D., … Tranel, P. J. (2018). Glyphosate-Resistant Junglerice (Echinochloa colona) from Mississippi and Tennessee: Magnitude and Resistance Mechanisms. *Weed Science*, *66*(5), 603–610. https://doi.org/10.1017/wsc.2018.51

Newman, M. M., Hoilett, N., Lorenz, N., Dick, R. P., Liles, M. R., Ramsier, C., & Kloepper, J. W. (2016). Glyphosate effects on soil rhizosphere-associated bacterial communities. *Science of the Total Environment*, *543*(2016), 155–160. https://doi.org/10.1016/j.scitotenv.2015.11.008

Pérez, G.L., Torremorell, A., Mugni, H., Rodriguez, P., Rodriguez, R., Vera, M. S., … Zagarese, A. H. (2007). *EFFECTS OF THE HERBICIDE ROUNDUP ON FRESHWATER MICROBIAL COMMUNITIES: A MESOCOSM STUDY*. *Ecological Applications* (Vol. 17).

Pérez, Gonzalo L., Vera, M. S., & Miranda, L. A. (2011). Effects of Herbicide Glyphosate and Glyphosate-Based Formulations on Aquatic Ecosystems. *Herbicides and the Environment*, 343–368. https://doi.org/ISBN: 978-953-307-476-4

Pizarro, H., Di Fiori, E., Sinistro, R., Ramírez, M., Rodríguez, P., Vinocur, A., & Cataldo, D. (2016). Impact of multiple anthropogenic stressors on freshwater: how do glyphosate and the invasive

mussel Limnoperna fortunei affect microbial communities and water quality? *Ecotoxicology*, *25*(1), 56–68. https://doi.org/10.1007/s10646-015-1566-x

PMRA. (2017). Re-evaluation decision RVD2017-01, Glyphosate. Ottawa, ON, Canada: Health Canada, Pest Management Regulatory Agency.

Pollegioni, L., Schonbrunn, E., & Siehl, D. (2011). Molecular basis of glyphosate resistance - Different approaches through protein engineering. *FEBS Journal*, *278*(16), 2753–2766. https://doi.org/10.1111/j.1742-4658.2011.08214.x

Powell, H. A., Kerbby, N. W., & Rowell, P. (1991). Natural tolerance of cyanobacteria to the herbicide glyphosate. *New Phytologist*, *119*(3), 421–426. https://doi.org/10.1111/j.1469-8137.1991.tb00042.x

Primost, J. E., Marino, D. J. G., Aparicio, V. C., Costa, J. L., & Carriquiriborde, P. (2017). Glyphosate and AMPA, "pseudo-persistent" pollutants under real-world agricultural management practices in the Mesopotamic Pampas agroecosystem, Argentina. *Environmental Pollution*. https://doi.org/10.1016/j.envpol.2017.06.006

Roberto, A. A., Van Gray, J. B., & Leff, L. G. (2018). Sediment bacteria in an urban stream: Spatiotemporal patterns in community composition. *Water Research*, *134*, 353–369. https://doi.org/10.1016/j.watres.2018.01.045

Robichaud, C. D., & Rooney, R. C. (2021). Effective suppression of established invasive Phragmites australis leads to secondary invasion in a coastal marsh . *Invasive Plant Science and Management*, 1–11. https://doi.org/10.1017/inp.2021.2

Rodriguez-Gil, J. L., Lissemore, L., Solomon, K., & Hanson, M. (2016). Dissipation of a commercial mixture of polyoxyethylene amine surfactants in aquatic outdoor microcosms: Effect of water depth and sediment organic carbon. *Science of the Total Environment*, *550*, 449–458. https://doi.org/10.1016/j.scitotenv.2016.01.140

Romaní, A. M., Guasch, H., Muñoz, I., Ruana, J., Vilalta, E., Schwartz, T., … Sabater, S. (2004). Biofilm structure and function and possible implications for riverine DOC dynamics. *Microbial Ecology*, *47*(4), 316–328. https://doi.org/10.1007/s00248-003-2019-2

Sayers, E. W., Cavanaugh, M., Clark, K., Ostell, J., Pruitt, K. D., & Karsch-Mizrachi, I. (2019). GenBank. *Nucleic Acids Research*, *47*(D1), D94–D99. https://doi.org/10.1093/nar/gky989

Schmidt, P. J., Cameron, E. S., Müller, K. M., & Emelko, M. B. (2021). Ensuring that fundamentals of quantitative microbiology are reflected in microbial diversity analyses based on next-generation sequencing. *BioRxiv*, 2021.06.19.449110. Retrieved from https://www.biorxiv.org/content/10.1101/2021.06.19.449110v1%0Ahttps://www.biorxiv.org/content/10.1101/2021.06.19.449110v1.abstract

Schoch, C. L., Ciufo, S., Domrachev, M., Hotton, C. L., Kannan, S., Khovanskaya, R., … Karsch-Mizrachi, I. (2020). NCBI Taxonomy: A comprehensive update on curation, resources and tools. *Database*, *2020*(2), 1–21. https://doi.org/10.1093/database/baaa062

Steinrucken, H.C. & Amrhein, N. (1980). The herbicide glyphosate is a potent inhibitor of 5-enolpyruvyl-shikimic acid-3-phosphate synthase. *Biochemical and Biophysical Research Communications*, *94*(4), 1207–1212.

Stosiek, N., Talma, M., & Klimek-Ochab, M. (2020). Carbon-Phosphorus Lyase - the State of the Art. *Applied Biochemistry and Biotechnology*, *190*, 1525–1552. https://doi.org/https://doi.org/10.1007/s12010-019-03161-4

Sviridov, A. V., Shushkova, T. V., Ermakova, I. T., Ivanova, E. V., Epiktetov, D. O., & Leont'evskii, A. A. (2015). Microbial Degradation of Glyphosate Herbicides (Review). *Прикладная Биохимия И Микробиология*, *51*(2), 183–190. https://doi.org/10.7868/S0555109915020221

Szekacs, A., & Darvas, B. (2012). *Forty Years with Glyphosate*. *Herbicides - Properties, Synthesis and Control of Weeds*. https://doi.org/10.5772/32491

Tani, E., Chachalis, D., & Travlos, I. S. (2015). A Glyphosate Resistance Mechanism in Conyza canadensis Involves Synchronization of EPSPS and ABC-transporter Genes. *Plant Molecular Biology Reporter*, *33*(6), 1721–1730. https://doi.org/10.1007/s11105-015-0868-8

Tohge, T., Watanabe, M., Hoefgen, R., & Fernie, A. R. (2013). Shikimate and Phenylalanine Biosynthesis in the Green Lineage. *Frontiers in Plant Science*, *4*(March), 1–13. https://doi.org/10.3389/fpls.2013.00062

Tsui, M. T. K., & Chu, L. M. (2003). Aquatic toxicity of glyphosate-based formulations: comparison between different organisms and the effects of environmental factors. *Chemosphere*, *52*, 1189–1197. https://doi.org/doi:10.1016/S0045-6535(03)00306-0

Vadeboncoeur, Y., & Power, M. E. (2017). Attached Algae: The Cryptic Base of Inverted Trophic

Pyramids in Freshwaters. *Annual Review of Ecology, Evolution, and Systematics*, *48*, 255–279. https://doi.org/10.1146/annurev-ecolsys-121415-032340

Van Bruggen, A. H. C., He, M. M., Shin, K., Mai, V., Jeong, K. C., Finckh, M. R., & Morris, J. G. (2018). Environmental and health effects of the herbicide glyphosate. *Science of the Total Environment*, *616–617*, 255–268. https://doi.org/10.1016/j.scitotenv.2017.10.309

Vera, M. S., Juárez, Á. B., & Pizarro, H. N. (2014). Comparative effects of technical-grade and a commercial formulation of glyphosate on the pigment content of periphytic algae. *Bulletin of Environmental Contamination and Toxicology*. https://doi.org/10.1007/s00128-014-1355-x

Vera, M. S., Lagomarsino, L., Sylvester, M., Gonzalo, •, Pérez, L., Rodríguez, P., … Pizarro, H. (2009). New evidences of Roundup Ò (glyphosate formulation) impact on the periphyton community and the water quality of freshwater ecosystems. https://doi.org/10.1007/s10646-009-0446-7

Wahl, M. (1989). Marine epibiosis. I. Fouling and antifouling: some basic aspects (review). *Marine Ecology Progress Series*, *58*, 175–189. https://doi.org/10.3354/meps058175

Waltz, E. (2010). Glyphosate resistance threatens Roundup hegemony. *Nature Biotechnology*, *28*(6), 537–539.

Wang, H., Bier, R., Zgleszewski, L., Peipoch, M., Omondi, E., Mukherjee, A., … Kan, J. (2020). Distinct Distribution of Archaea From Soil to Freshwater to Estuary: Implications of Archaeal Composition and Function in Different Environments. *Frontiers in Microbiology*, *11*(October). https://doi.org/10.3389/fmicb.2020.576661

Wu, Y. (2017). Periphyton. *Periphyton*, 225–249. https://doi.org/10.1016/B978-0-12-801077-8.00009-0

Appendix A

Site and Lab Photos

Figure 11: Photos of 2018 site locations at collection. U-poles with flagging tape and some buoys are visible. (A- RT1; B- RT10; C- RT15; D- RTA; E- RTB; F- RTE).

Figure 12: Photos of 2018 lab set up. Control microcosms are on the upper shelf while treatment microcosms are on the lower shelf. (A- Shelves holding microcosms with lights and pumps on; B- Treatment microcosms viewed from above; C- close view of plates in microcosm from above).
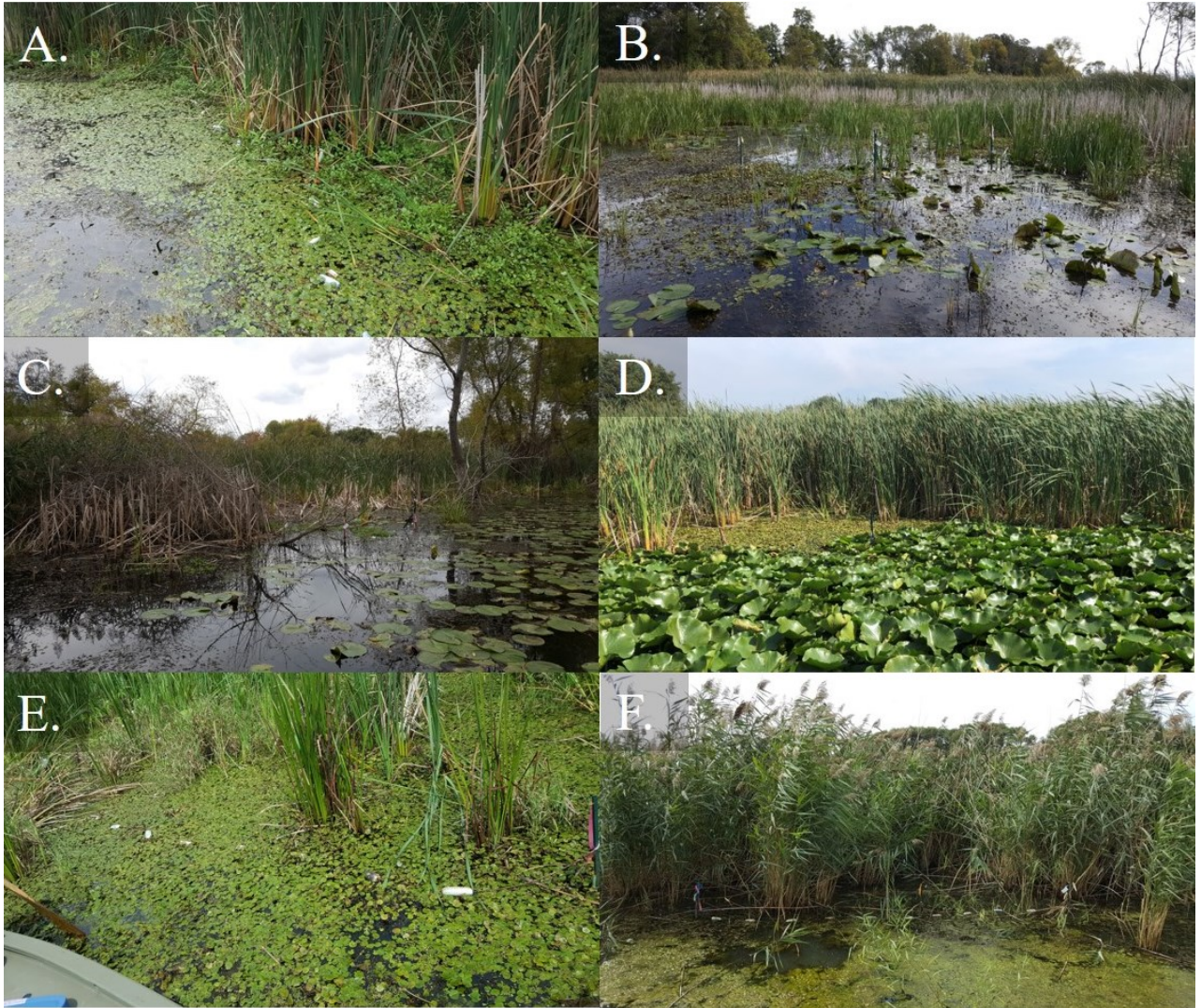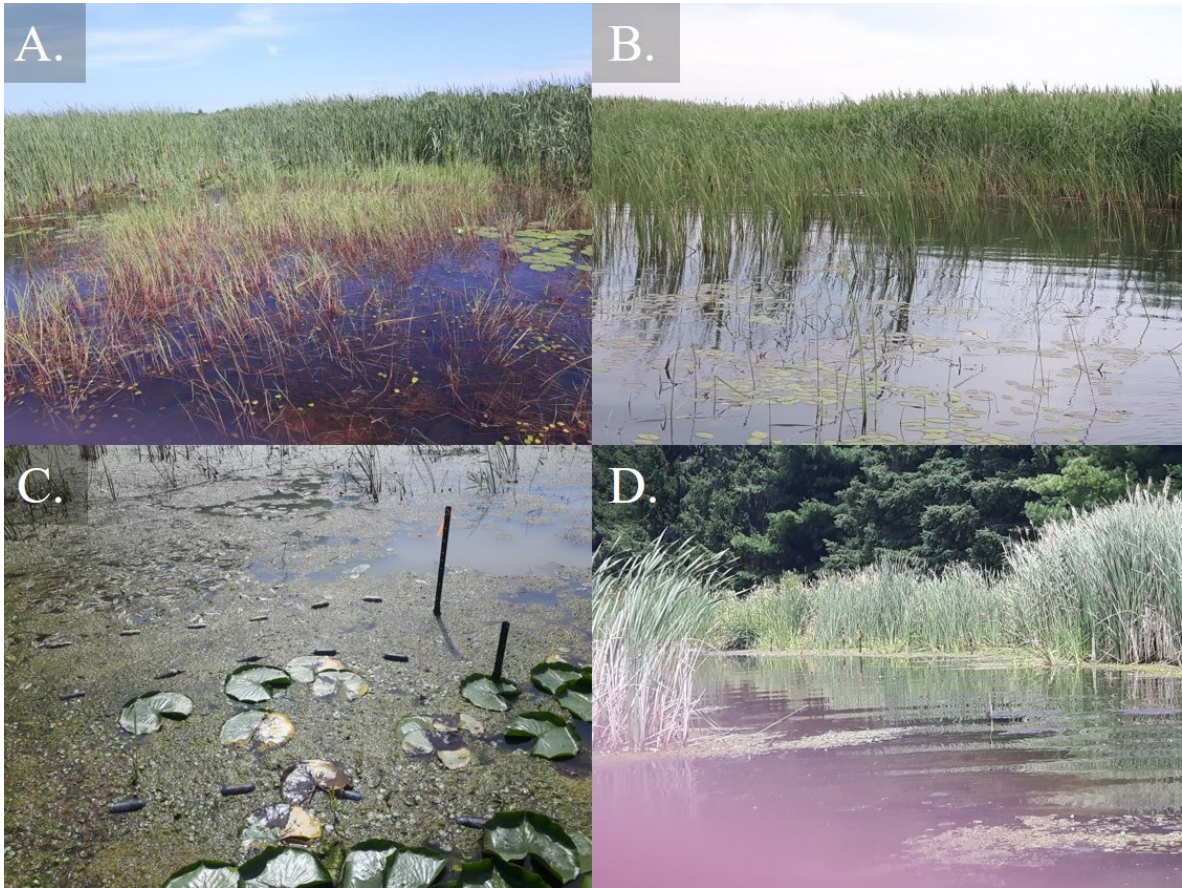
Figure 13: Photos of 2019 site locations at collection. U-poles with flagging tape and some buoys are visible. (A- RLP; B- RSP; C- RT10; D- RTB).
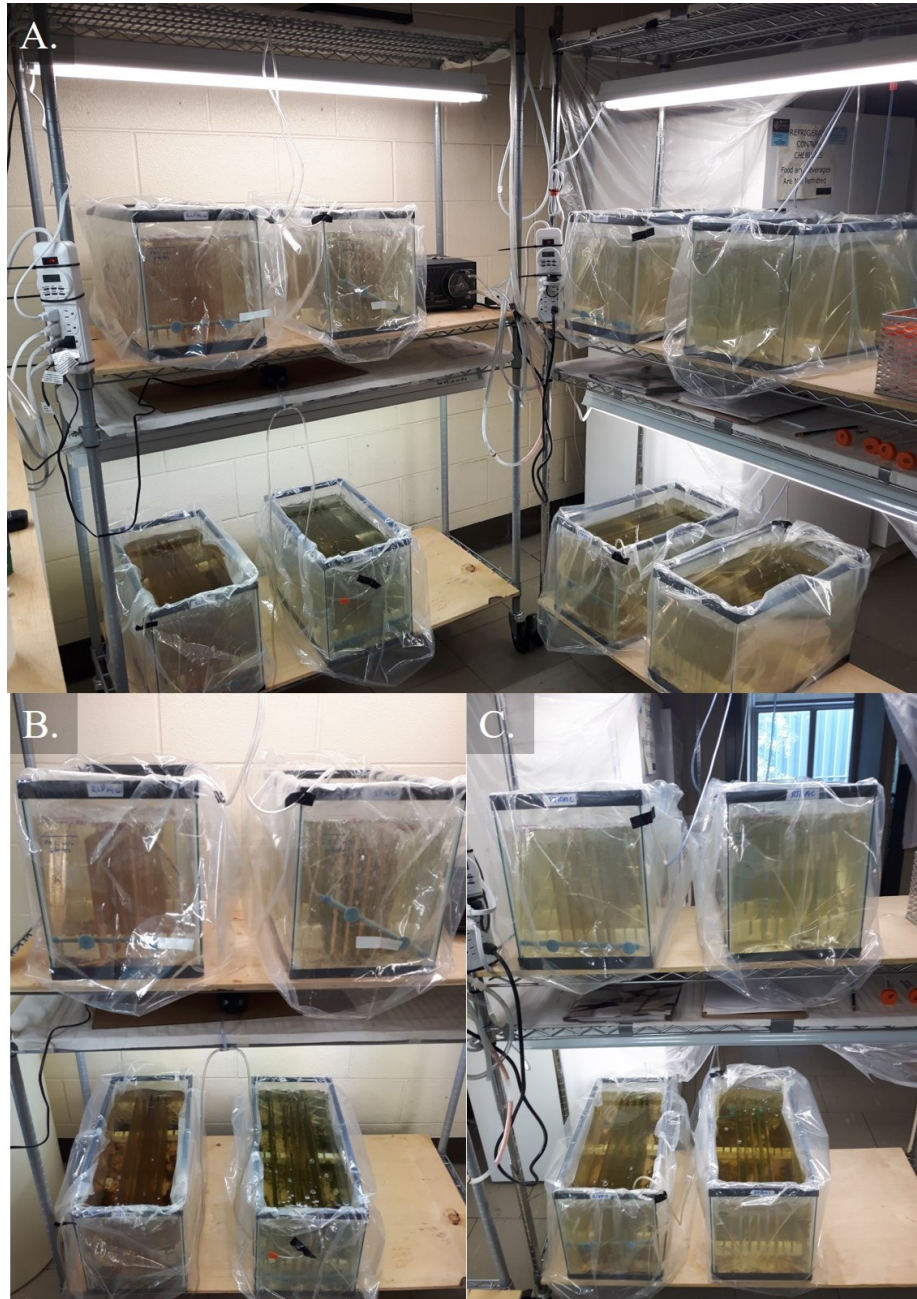
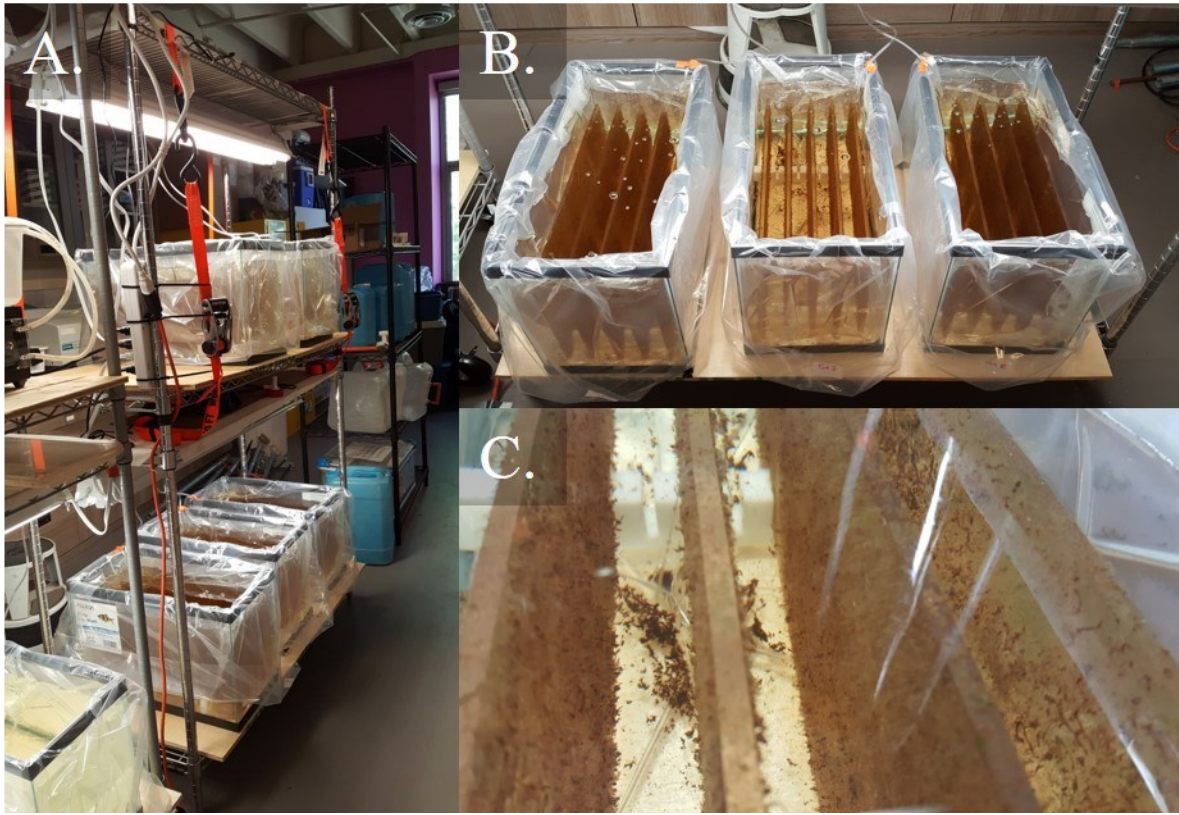Figure 14: Photos of 2019 lab set up. Control microcosms are on the upper shelves while treatment microcosms are on the lower shelves. (A- All microcosms set up under normal lab conditions, RLP and RSP are on the left shelving unit, while RT10 and RTB are on the righthand unit; B- RLP and RSP microcosms; C- RT10 and RTB microcosms).

Figure 15: Photo of biofilm collection and transportation setup.

Appendix B

Site Characteristics

Table 10: Summary of site characteristics, GPS coordinates, and environmental conditions for the *in situ* colonization of biofilms.

|		Riverine Wetland Sites 2018						Riverine Wetland Sites 2019		Lacustrine Wetland Sites 2019	
		RTA	RTB	RT1	RTE	RT10	RT15	RT10	RTB	RLP	RSP
Site Coordinates	**Latitude**	42.3337	42.3336	42.3355	42.2769	42.3127	42.2934	42.3135	42.3336	42.2580	42.2609
	Longitude	-81.8553	-81.8592	-81.8463	-81.9392	-81.9012	-81.9305	-81.9016	-81.8591	-81.8745	-81.8757
***In situ* Water Chemistry at collection**	**AMPA (µg/L)**	0	0	0	0	0	0	4	4	0	0
	Glyphosate (µg/L)	0	0	0	0	0	0	25	0	0	0
Site Characteristics — **Installation**	**Date**	24-May-18	24-May-18	24-May-18	23-May-18	23-May-18	23-May-18	31-May-19	31-May-19	31-May-19	31-May-19
	Water depth (cm)*	96 (± 5)	87 (± 2)	101 (± 6)	71 (± 8)	55 (± 1)	76 (± 5)	94 (± 7)	101 (± 8)	88 (± 7)	113 (± 6)
	Water temp (˚C)	22.3	23.0	22.8	20.1	22.3	20.8	20.9	20.8	18.7	20.4
	Conductivity (ppt)	0.29	0.28	0.19	0.32	0.32	0.31	0.29	0.57	0.07	0.14
Collection	**Date**	27-Aug-18	27-Aug-18	27-Aug-18	27-Sep-18	27-Sep-18	27-Sep-18	18-Jul-19	18-Jul-19	18-Jul-19	18-Jul-19
	Water depth (cm)*	74 (± 0)	91 (± 3)	71 (± 0)	82 (± 6)	62 (± 10)	81 (± 1)	95 (± 10)	104 (± 7)	100 (± 6)	119 (± 6)
	Water temp (˚C)	27.8	25.1	24.6	20.1	16.7	19.0	24.9	26.6	29.9	29
	Conductivity (ppt)	0.13	0.15	0.14	0.22	0.25	0.30	0.19	0.22	0.13	0.11
	Dissolved O_2 (mg/L)**	3.54	6.25	4.48	6.75	6.37	7.54	1.43	2.11	1.98	n/a

	Riverine Wetland Sites 2018						Riverine Wetland Sites 2019		Lacustrine Wetland Sites 2019	
	RTA	**RTB**	**RT1**	**RTE**	**RT10**	**RT15**	**RT10**	**RTB**	**RLP**	**RSP**
Surrounding Vegetation	frogbit, large waterlilies, *Typha*	burreed, duckweed, frogbit, reed canary grass, surface algae/scum, *Typha*	frogbit, Phragmites, surface algae/scum, *Typha*, unidentified submerged aquatic vegetation	Duckweed, frogbit, *Phragmites*, submerged aquatic vegetation, surface algae/scum, unidentified emergent leafy vegetation	frogbit, large waterlilies, submerged aquatic vegetation, *Typha*, unidentified rush species	frogbit, large waterlilies, submerged aquatic vegetation, *Typha*, unknown emergent leafy macrophyte	frogbit, large waterlilies, surface algae/scum	frogbit, large waterlilies, *Phragmites*, *Typha*	Carex, frogbit, large waterlilies, *Phragmites*, *Typha*	*Phragmites, Typha*
Visual Description of Water	cloudy/ turbid	cloudy/ turbid	cloudy/ turbid	not recorded	not recorded	not recorded	cloudy/ turbid	cloudy/ turbid	clear	clear

63

Table 11: Summary of all samples collected from the microcosms for the duration of the experiment.

Sample	*in situ*	Week 1	Week 2	Week 3	Week 4
Field Collection					
Glyphosate dose					
Glyphosate/AMPA sample					
Total phosphorus (TP) sample					
Soluble reactive phosphorus (SRP) sample					
Total nitrogen sample					
Ammonia sample					
Nitrate/Nitrite sample					
Diving PAM					
AFDM sample					
Chlorophyll a sample					
Genetic sample					
Microscope sample					
Water condition measurements					
Water exchange					
1 hr post dose glypho/AMPA sample					
1 hr post dose TP sample					
1 hr post dose SRP sample					
Filter SRP					

Sample	*in situ*				Week 1					Week 2					Week 3				Week 4		
Filter NH4 and NO3/NO2																					
Filter chlorophyll a																					

Appendix D

Study Design Variation Summary Table

Table 12: Summary table of the variation between study design in 2018 and 2019. Including calculations for glyphosate exposure concentrations.

Variable	2018	2019
Number of Sites	6	4
Site Type	All riverine wetlands	Two riverine and two lacustrine wetlands
Collection Schedule	RTA, RTB, and RT1: August 27, 2018 RTE, RT10, and RT15: September 27, 2018	All collected July 18, 2019
Site Codes	RTA, RTB, RTE, RT1, RT10, RT15	RTB, RT10, RLP, RSP
Microcosm Volume	27L	28L
Glyphosate Exposure Calculation	[480 mg/L * 0.028125 L] / [27 L] = 0.5 mg a.e./L	[480 mg/L * 0.02917 L] / [28 L] = 0.5 mg a.e./L

Appendix E

Raw ASV Reads

Raw ASV reads are available in fastq.gz file formats at DOI: 10.6084/m9.figshare.16987873

Appendix F

Filtered ASV Summary Table

Full table of ASV counts after filtering by MetagenomBio Inc., as well as proportionate reads calculated for use in PCORD are available at DOI: 10.6084/m9.figshare.17035481.

Appendix G

Shannon-Weiner Diversity Analysis and Richness Calculations

Full summary of Shannon-Weiner Diversity Index and Richness from rarefying code and additional supplementary calculations for Table 3 are available at DOI: 10.6084/m9.figshare.17012252.

Full Two-Way ANOVA results available at DOI: 10.6084/m9.figshare.17012252.

Appendix H

Blocked ISA Results

Full blocked ISA table is available at DOI: 10.6084/m9.figshare.17035490.

Appendix I

EPSPS and C-P Lyase BLAST Sequences

EPSPS BLAST Sequence

>sp|P0A6D3|AROA_ECOLI 3-phosphoshikimate 1-carboxyvinyltransferase OS=Escherichia coli (strain K12) OX=83333 GN=aroA PE=1 SV=1

MESLTLQPIARVDGTINLPGSKSVSNRALLLAALAHGKTVLTNLLDSDDVRHMLNALTAL

GVSYTLSADRTRCEIIGNGGPLHAEGALELFLGNAGTAMRPLAAALCLGSNDIVLTGEPR

MKERPIGHLVDALRLGGAKITYLEQENYPPLRLQGGFTGGNVDVDGSVSSQFLTALLMTA

PLAPEDTVIRIKGDLVSKPYIDITLNLMKTFGVEIENQHYQQFVVKGGQSYQSPGTYLVE

GDASSASYFLAAAAIKGGTVKVTGIGRNSMQGDIRFADVLEKMGATICWGDDYISCTRGE

LNAIDMDMNHIPDAAMTIATAALFAKGTTTLRNIYNWRVKETDRLFAMATELRKVGAEVE

EGHDYIRITPPEKLNFAEIATYNDHRMAMCFSLVALSDTPVTILDPKCTAKTFPDYFEQL

ARISQAA

C-P Lyase BLAST Sequences

>phnA_AKA:yjdM,ECK4101_E.coli_NC_000913.3:c4326734-4326399 Escherichia coli str. K-12 substr. MG1655, complete genome

MSLPHCPKCNSEYTYEDNGMYICPECAYEWNDAEPAQESDELIV

KDANGNLLADGDSVTIIKDLKVKGSSSMLKIGTKVKNIRLVEGDHNIDCKIDGFGPMK

LKSEFVKKN

>phnB_AKA:yjdN,ECK4100_E.coli_NC_000913.3:c4325741-4325298 Escherichia coli str. K-12 substr. MG1655, complete genome

MYTQTLYELSQEAERLLQLSRQQLQLLEKMPLSVPGDDAPQLAL

PWSQPNIAERHAMLNNELRKISRLEMVLAIVGTMKAGKSTTINAIVGTEVLPNRNRPM

TALPTLIRHTPGQKEPVLHFSHVAPIDCLIQQLQQRLRDCDIKHLTDVLEIDKDMRAL

MQRIENGVAFEKYYLGAQPIFHCLKSLNDLVRLAKALDVDFPFSAYAAIEHIPVIEVE

FVHLAGLESYPGQLTLLDTPGPNEAGQPHLQKMLNQQLARASAVLAVLDYTQLKSISD

EEVREAILAVGQSVPLYVLVNKFDQQDRNSDDADQVRALISGTLMKGCITPQQIFPVS

SMWGYLANRARYELANNGKLPPPEQQRWVEDFAHAALGRRWRHADLADLEHIRHAADQ

LWEDSLFAQPIQALLHAAYANASLYALRSAAHKLLNYAQQAREYLDFRAHGLNVACEQ

LRQNIHQIEESLQLLQLNQAQVSGEIKHEIELALTSANHFLRQQQDALKVQLAALFQD

DSEPLSEIRTRCETLLQTAQNTISRDFTLRFAELESTLCRVLTDVIRPIEQQVKMELS

ESGFRPGFHFPVFHGVVPHFNTRQLFSEVISRQEATDEQSTRLGVVRETFSRWLNQPD

WGRGNEKSPTETVDYSVLQRALSAEVDLYCQQMAKVLAEQVDESVTAGMNTFFAEFAS

CLTELQTRLRESLALRQQNESVVRLMQQQLQQTVMTHGWIYTDAQLLRDDIQTLFTAE

RY

>phnC_E.coli_NC_000913.3:c4325165-4324377 Escherichia coli str. K-12 substr. MG1655, complete genome
MQTIIRVEKLAKTFNQHQALHAVDLNIHHGEMVALLGPSGSGKS

TLLRHLSGLITGDKSVGSHIELLGRTVQREGRLARDIRKSRAHTGYIFQQFNLVNRLS

VLENVLIGALGSTPFWRTCFSWFTGEQKQRALQALTRVGMVHFAHQRVSTLSGGQQQR

VAIARALMQQAKVILADEPIASLDPESARIVMDTLRDINQNDGITVVVTLHQVDYALR

YCERIVALRQGHVFYDGSSQQFDNERFDHLYRSINRVEENAKAA

>phnD_E.coli_NC_000913.3:c4324352-4323336 Escherichia coli str. K-12 substr. MG1655, complete genome
MNAKIIASLAFTSMFSLSTLLSPAHAEEQEKALNFGIISTESQQ

NLKPQWTPFLQDMEKKLGVKVNAFFAPDYAGIIQGMRFNKVDIAWYGNLSAMEAVDRA

NGQVFAQTVAADGSPGYWSVLIVNKDSPINNLNDLLAKRKDLTFGNGDPNSTSGFLVP

GYYVFAKNNISASDFKRTVNAGHETNALAVANKQVDVATNNTENLDKLKTSAPEKLKE

LKVIWKSPLIPGDPIVWRKNLSETTKDKIYDFFMNYGKTPEEKAVLERLGWAPFRASS

DLQLVPIRQLALFKEMQGVKSNKGLNEQDKLAKTTEIQAQLDDLDRLNNALSAMSSVS

KAVQ

>phnE_E.coli_NC_000913.3:c4323281-4322443 Escherichia coli str. K-12 substr. MG1655, complete genome

MPDAVQAPYP AYRPEPNMQT ITIAPPKRSW FSLLSWAVVL AVLVVSWQGA

EMAPLTLIKD GGNMATFAAD FFPPDFSQWQ DYLTEMAVTL QIAVWGTALA

VVLSIPFGLM SAENLVPWWV YQPVRRLMDA CRAINEMVFA MLFVVAVGLG

PFAGVLACWR CLSTPPACSP SCFPKRWKRL SPARWKAFAP PVPTSSKRSS

TACCHR

>phnF_E.coli_NC_000913.3:c4322422-4321697 Escherichia coli str. K-12 substr. MG1655, complete genome

MHLSTHPTSYPTRYQEIAAKLEQELRQHYRCGDYLPAEQQLAAR

FEVNRHTLRRAIDQLVEKGWVQRRQGVGVLVLMRPFDYPLNAQARFSQNLLDQGSHPT

SEKLLSVLRPASGHVADALGITEGENVIHLRTLRRVNGVALCLIDHYFADLTLWPTLQ

RFDSGSLHDFLREQTGIALRRSQTRISARRAQAKECQRLEIPNMSPLLCVRTLNHRDG

ESSPAEYSVSLTRADMIEFTMEH

>phnG_E.coli_NC_000913.3:c4321696-4321244 Escherichia coli str. K-12 substr. MG1655, complete genome

MHADTATRQHWMSVLAHSQPAELAARLNALNITADYEVIRAAET

GLVQIQARMGGTGERFFAGDATLTRAAVRLTDGTLGYSWVQGRDKQHAERCALIDALM

QQSRHFQNLSETLIAPLDADRMARIAARQAEVNASRVDFFTMVRGDNA

>phnH_E.coli_NC_000913.3:c4321247-4320663 Escherichia coli str. K-12 substr. MG1655, complete genome

73

MTLETAFMLPVQDAQHSFRRLLKAMSEPGVIVALHQLKRGWQPL

NIATTSVLLTLADNDTPVWLSTPLNNDIVNQSLRFHTNAPLVSQPEQATFAVTDEAIS

SEQLNALSTGTAVAPEAGATLILQVASLSGGRMLRLTGAGIAEERMIAPQLPECILHE

LTERPHPFPLGIDLILTCGERLLAIPRTTHVEVC

>phnI_E.coli_NC_000913.3:c4320663-4319599 Escherichia coli str. K-12 substr. MG1655, complete genome

MYVAVKGGEKAIDAAHALQESRRRGDTDLPELSVAQIEQQLNLA

VDRVMTEGGIADRELAALALKQASGDNVEAIFLLRAYRTTLAKLAVSEPLDTTGMRLE

RRISAVYKDIPGGQLLGPTYDYTHRLLDFTLLANGEAPTLTTADSEQQPSPHVFSLLA

RQGLAKFEEDSGAQPDDITRTPPVYPCSRSSRLQQLMRGDEGYLLALAYSTQRGYGRN

HPFAGEIRSGYIDVSIVPEELGFAVNVGELLMTECEMVNGFIDPPGEPPHFTRGYGLV

FGMSERKAMAMALVDRALQAPEYGEHATGPAQDEEFVLAHADNVEAAGFVSHLKLPHY

VDFQAELELLKRLQQEQNHG

>phnJ_E.coli_NC_000913.3:c4319606-4318761 Escherichia coli str. K-12 substr. MG1655, complete genome

MANLSGYNFAYLDEQTKRMIRRAILKAVAIPGYQVPFGGREMPM

PYGWGTGGIQLTASVIGESDVLKVIDQGADDTTNAVSIRNFFKRVTGVNTTERTDDAT

VIQTRHRIPETPLTEDQIIIFQVPIPEPLRFIEPRETETRTMHALEEYGVMQVKLYED

IARFGHIATTYAYPVKVNGRYVMDPSPIPKFDNPKMDMMPALQLFGAGREKRIYAVPP

FTRVESLDFDDHPFTVQQWDEPCAICGSTHSYLDEVVLDDAGNRMFVCSDTDYCRQQS

EAKNQ

>phnK_E.coli_NC_000913.3:c4318764-4318006 Escherichia coli str. K-12 substr. MG1655, complete genome

MNQPLLSVNNLTHLYAPGKGFSDVSFDLWPGEVLGIVGESGSGK

TTLLKSISARLTPQQGEIHYENRSLYAMSEADRRRLLRTEWGVVHQHPLDGLRRQVSA

GGNIGERLMATGARHYGDIRATAQKWLEEVEIPANRIDDLPTTFSGGMQQRLQIARNL
VTHPKLVFMDEPTGGLDVSVQARLLDLLRGLVVELNLAVVIVTHDLGVARLLADRLLV
MKQGQVVESGLTDRVLDDPHHPYTQLLVSSVLQN
>phnL_E.coli_NC_000913.3:c4317895-4317215 Escherichia coli str. K-12 substr. MG1655, complete genome
MINVQNVSKTFILHQQNGVRLPVLNRASLTVNAGECVVLHGHSG
SGKSTLLRSLYANYLPDEGQIQIKHGDEWVDLVTAPARKVVEIRKTTVGWVSQFLRVI
PRISALEVVMQPLLDTGVPREACAAKAARLLTRLNVPERLWHLAPSTFSGGEQQRVNI
ARGFIVDYPILLLDEPTASLDAKNSAAVVELIREAKTRGAAIVGIFHDEAVRNDVADR
LHPMGASS
>phnM_E.coli_NC_000913.3:c4317218-4316082 Escherichia coli str. K-12 substr. MG1655, complete genome
MIINNVKLVLENEVVSGSLEVQNGEIRAFAESQSRLPEAMDGEG
GWLLPGLIELHTDNLDKFFTPRPKVDWPAHSAMSSHDALMVASGITTVLDAVAIGDVR
DGGDRLENLEKMINAIEETQKRGVNRAEHRLHLRCELPHHTTLPLFEKLVQREPVTLV
SLMDHSPGQRQFANREKYREYYQGKYSLTDAQMQQYEEEQLALAARWSQPNRESIAAL
CRARKIALASHDDATHAHVAESHQLGSVIAEFPTTFEAAEASRKHGMNVLMGAPNIVR
GGSHSGNVAASELAQLGLLDILSSDYYPASLLDAAFRVADDQSNRFTLPQAVKLVTKN
PAQALNLQDRGVIGEGKRADLVLAHRKDNHIHIDHVWRQGKRVF
>phnN_E.coli_NC_000913.3:c4316082-4315525 Escherichia coli str. K-12 substr. MG1655, complete genome
MMGKLIWLMGPSGSGKDSLLAELRLREQTQLLVAHRYITRDASA
GSENHIALSEQEFFTRAGQNLLALSWHANGLYYGVGVEIDLWLHAGFDVLVNGSRAHL
PQARARYQSALLPVCLQVSPEILRQRLENRGRENASEINARLARAARYTPQDCHTLNN
DGSLRQSVDTLLTLIHQKEKHHACL

\>phnO_E.coli_NC_000913.3:c4315538-4315104 Escherichia coli str. K-12 substr. MG1655, complete genome
MPACELRPATQYDTDAVYALICELKQAEFDHHAFRVGFNANLRD
PNMRYHLALLDGEVVGMIGLHLQFHLHHVNWIGEIQELVVMPQARGLNVGSKLLAWAE
EEARQAGAEMTELSTNVKRHDAHRFYLREGYEQSHFRFTKAL

\>phnP_E.coli_NC_000913.3:c4315102-4314344 Escherichia coli str. K-12 substr. MG1655, complete genome
MSLTLTLTGTGGAQGVPAWGCECAACARARRSPQYRRQPCSGVV
KFNDAITLIDAGLHDLADRWSPGSFQQFLLTHYHMDHVQGLFPLRWGVGDPIPVYGPP
DEQGCDDLFKHPGLLDFSHTVEPFVVFDLQGLQVTPLPLNHSKLTFGYLLETAHSRVA
WLSDTAGLPEKTLKFLRNNQPQVMVMDCSHPPRADAPRNHCDLNTVLALNQVIRSPRV
ILTHISHQFDAWLMENALPSGFEVGFDGMEIGVA

Appendix J

BLAST Results Summary Table

Full summary of NCBI BLAST results can be found at DOI: 10.6084/m9.figshare.17035493.

Appendix K

Glyphosate and AMPA Concentrations

Full summary of glyphosate and AMPA concentrations are available at DOI: 10.6084/m9.figshare.17035502